Coláiste na hOllscoile Corcaigh, Éire
University College Cork, Ireland

Assessment of the utility of the ESA SST CCI product for environmental research using data from meteorological buoys in the North Atlantic

Hannah Binner

BSCRES 4

Supervisors:

Dr Timothy Sullivan (School of BEES, UCC)

Rory Scarrott (Department of Geography, ERI, UCC)

Thesis submitted: 16th of March 2018

Contents

Acronym and abbreviation list	p.	3
Abstract	p.	4
1 Introduction	p.	5
2 Materials and Methods	p.	8
2.1 Study Area	p.	8
2.2 Satellite sensor data	p.	9
2.3 *In-situ* data	p.	12
2.4 Data processing	p.	13
3 Results	p.	16
4 Discussion	p.	30
5 Conclusions	p.	36
6 Recommendations	p.	36
7 Acknowledgements	p.	36
8 References	p.	37
Appendix	p.	40

Acronym and abbreviation list

AMSR	Advanced Microwave Scanning Radiometer
AOI	Area Of Interest
ATSR	Along-Track Scanning Radiometer
AVHRR	Advanced Very High Resolution Radiometer
CCI	Climate Change Initiative
CDR	Climate Data Record
CEDA	Centre for Environmental Data Analysis
ECVs	Essential Climate Variables
ESA	European Space Agency
ESA CCI	European Space Agency Climate Change Initiative
ESA SST CCI	European Space Agency Sea Surface Temperature Climate Change Initiative
GCOS	Global Climate Observing System
GHRSST	GODAE High-Resolution Sea Surface Temperature
GHRSST-PP	GODAE High-Resolution Sea Surface Temperature Pilot Project
GMPE	GHRSST Multi-Product Ensemble
GODAE	Global Ocean Data Assimilation Experiment
GTS	Global Telecommunication System
HadSST2	the Second Hadley Centre Sea Surface Temperature dataset
IQR	Interquartile range
IR	infrared
LOESS	Locally Weighted Scatterplot Smoother
MAWS	Marine Automatic Weather Station
MW	microwave
netCDF	Network Common Data Form
OI	Optimal Interpolation
OSTIA	Operational Sea Surface Temperature and Sea Ice Analysis
PCA	Principal Components Analysis
SD	Standard deviation
SST	Sea Surface Temperature
SST_{depth}	Sea Surface Temperature measurement at the specified depth
SST_{fnd}	Sea Surface Temperature measurement at foundation level
SST_{skin}	Sea Surface Temperature measurement at skin level
$SST_{sub\text{-}skin}$	Sea Surface Temperature measurement at sub-skin level
STFC	Science and Technology Facilities Council
WGS	World Geodetic System

Abstract

This study assessed the accuracy and utility of the European Space Agency's Sea Surface Temperature Climate Change Initiative (ESA SST CCI) product, which was established through the Global Ocean Data Assimilation Experiment (GODAE) and the GODAE High-Resolution SST Pilot-Project (GHRSST-PP). The product, the GHRSST Multi-product ensemble (GMPE), delivered Sea Surface Temperature (SST) measurements as a global daily median observation. These daily observations were aimed to be validated through the use of *in-situ* data, using four of the Met Éireann meteorological buoys. For the validation, the satellite images were processed in order to obtain the SST measurement that the satellite sensors had taken at the location of each of the four *in-situ* buoys and compared to the SST measurements taken by the *in-situ* buoys. Overall, satellite observations were found to have lower SST observations, while the buoy data showed a higher variability. Seasonal variability reflected in the satellite sensor and the buoy data. It was validated, that the satellite sensor data was accurate within 0.18 °C for the M3 buoy, 0.22 °C for the M6 buoy, 0.28 °C for the M5 buoy and 0.85 °C for the M4 buoy. It was also shown that the data was more reliable for summer months at the M3 and M5 buoy locations and least reliable for the M4 buoy location, which was attributed to a potential calibration error. Results of the M6 buoy location were attributed with a large uncertainty due to outliers.

The utility of the SST variable GMPE data for use in Irish waters is suggested for application in fisheries and aquaculture.

1. Introduction

Sea surface temperature (SST) is an important environmental parameter due to many of the world's systems depending on it, including marine and ocean ecosystems, ocean circulations, atmospheric water vapour, meteorological patterns and biodiversity (EPA, 2016). Research has shown that the oceans are warming: a study from the EPA (2016) detected a warming trend of 0.07 °C on average per decade between 1971 and 2000, while Cannaby and Hüsrevoglu (2009) have reported an average warming trend of 0.3 °C between 1850 and 2007. In terms of climate modelling, SST measurements are an important parameter for many model predictions (Atkinson *et al*., 2013). SST can be measured by satellite sensors due to the property of light to travel in waves. Each wavelength corresponds to a unique frequency; the magnitude of that frequency can be measured and any changes in magnitude can be attributed to a change in temperature. The wavelengths used to measure SST are infrared (3.55 to 12.5 μm) and microwave (6.9 to 89 GHz) due to their different attenuation length corresponding to a SST at a depth of a few millimetres, at microwave wavelength, and 20 micrometres, at infrared wavelength. Their unique properties are, that infrared measurements are available at high resolution and accuracy, but susceptible to cloud cover, while microwave measurements are available at a lower resolution, but capable to penetrate cloud cover due to the very low level microwave emission of clouds.

Sea surface temperature data is available from several sources: observations from drifting buoys and voluntary or research ships make up the earliest datasets, while satellite observations have created a long-term continuous dataset with global coverage. In past research, drifting buoy observations were often found to suffer from gross errors, while ship observations were found to have more diverse errors and be less reliable due to recalibration of instruments, if not failure of instruments, causing disruptions in the collectable data (Atkinson *et al*., 2013). Another major drawback in the available data was the availability of data subject to shipping routes and drifting buoy positioning, all of which was remedied through the introduction of satellite sensor data, which is capable of obtaining global images at daily to weekly temporal resolutions. However, optimisation of satellite instruments is ongoing. In the past 20 years, there were several projects committed to establishing long-term continuous and reliable SST datasets, such as the Second Hadley Centre Sea Surface Temperature (HadSST2) dataset (Rayner, et al., 2006), the GODAE GHRSST-PP (GHRSST Science Team, 2010) and the Operational Sea Surface Temperature and Sea Ice Analysis

(OSTIA). Due to satellite sensor data showing a certain degree of uncertainty associated with several factors such as cloud cover, presence of aerosols, diurnal variations, sensor or satellite drift, these datasets often applied an algorithm and/ or reference dataset.

When in 2002, the Global Ocean Data Assimilation Experiment (GODAE) was established with the premise of improving satellite sensor accuracy, which at the time was found to be 0.4 K (0.4 °C) for SST satellite sensor products, the process of improving model performances for SST observations started (Donlon, *et al*., 2007). In 2007, the GODAE High-Resolution SST Pilot Project (GHRSST-PP) followed, which then progressed to the European Space Agency SST Climate Change Initiative (ESA SST CCI) with the premise to fulfil the requirements of an Essential Climate Variable (ECV) as set out by the Global Climate Observing System (GCOS) of producing long-term SST datasets with an accuracy performance improvement of 0.1 K (0.1 °C). One of the products resulting from the ESA SST CCI was the GHRSST Multi-product ensemble (GMPE), which was a Level 4 product that produced global daily blended images of a median SST; the specifics of each of the terms will be explained in the following. This product was examined and aimed to be validated in this study. In detail, the GMPE produced one daily image with global coverage. It is a blended product, because it blends the SST measurements obtained by the Advanced Very High Resolution Radiometer (AVHRR) sensor, measured at infrared wavelengths between 3.55 and 12.50 µm (NOAASIS, 2017), the Along Track Scanning Radiometer (ATSR) sensors, ATSR-1, ATSR-2 and AATSR, also measured at infrared wavelengths between 3.7 and 12.0 µm (Veal and Corlett, 2017) and the Advanced Microwave Scanning Radiometer (AMSR) sensor, AMSR-E, measured by microwave wavelengths between 6.93 and 89.0 GHz (Veal and Corlett, 2017), and computes the median value of all measurements, for each pixel, as a measure of SST at approximately 20 cm depth (STFC, 2011a). In order to achieve an accurate representation of the sea surface temperature at 20 cm depth, the current scientific understanding of the vertical near surface thermal stratification was taken into account, corrected for and associated uncertainty applied (GHRSST, 2018; Merchant, *et al*., 2014a), which will be explained further in Section 2.2 of this paper. Figure 1 illustrates the differences in depth, at which the measurements were taken, further. While the infrared satellite sensors measurement depths correspond to a SST_{skin} depth, the microwave satellite sensor measurement depth corresponds to a $SST_{sub\text{-}skin}$ depth, as is illustrated by A in Figure 1, and their median corresponds to a SST_{depth} measurement, as is illustrated by B in Figure 1.

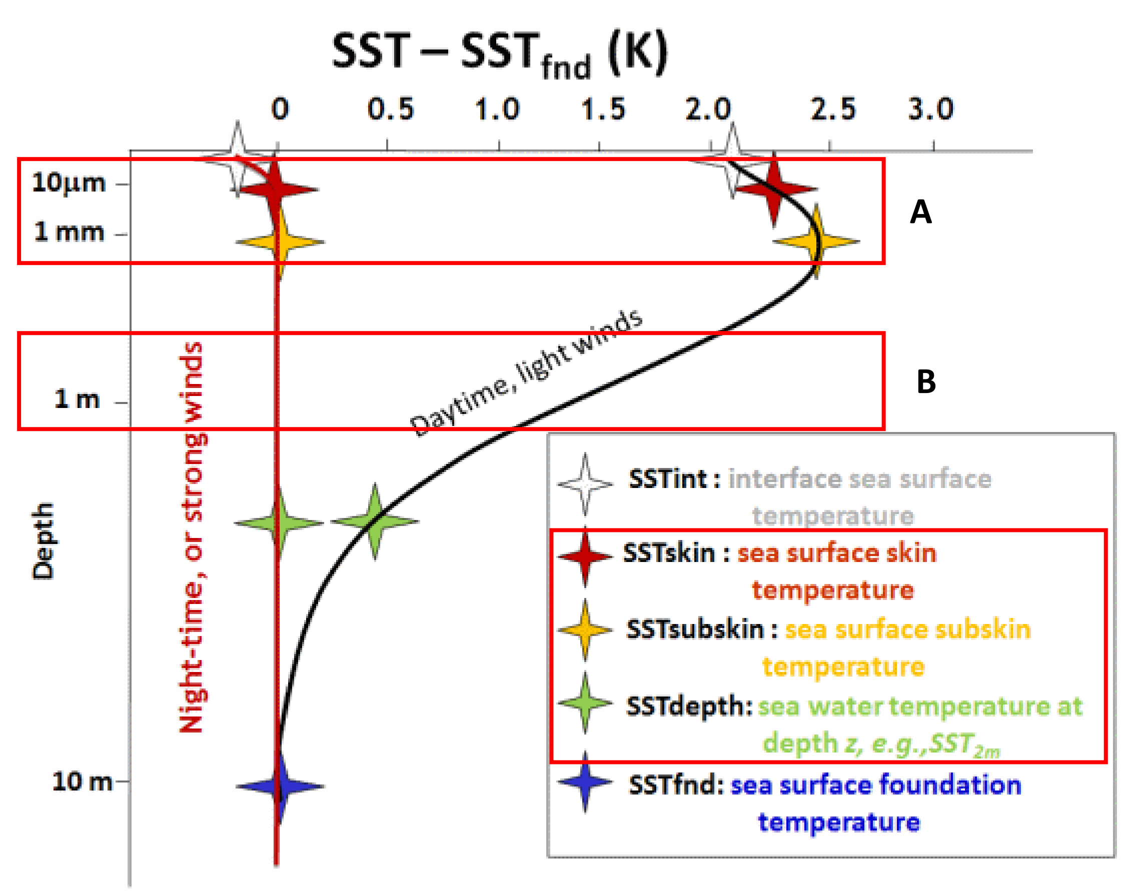

Fig. 1: Schematic diagram showing a vertical temperature profile through the ocean surface layer during (a) night time and (b) day time with solar heating (source: GHRSST, 2018).

The median is referred to as an ensemble median because it is computed taking into account the anomaly of each ensemble member from the median (STFC, 2011b). The Level 4 (L4) product combines observations from all the sensors and combines it with the optimal interpolation (OI) systems (GHRSST, 2018; STFC, 2011a); optimal interpolation is described further in Section 2.2 of this paper.

The objectives of this study were to validate the accuracy of this product, the GMPE Level 4 product, using buoy measurements and to show the applicability of the dataset to research in environmental science. The buoy measurement that were used for validation in this study were the M3, M4, M5 and M6 Met Éireann meteorological buoys. Their SST measurements, taken at 1m depth, correspond to an SST_{depth} measurement, as is illustrated by B in Figure 1. In validating the accuracy of the dataset, as it is provided through the ESA CCI project, its application within research gains importance as it then can be readily used to examine correlations with other environmental parameters.

2. Materials and Methods

Changes in sea surface temperature were assessed using the European Space Agency's Climate Change Initiative Sea Surface Temperature (ESA CCI SST) Level 4 GHRSST Multi-Product Ensemble (GMPE) product; a product that combines Along-track Scanning Radiometer (ATSR), Advanced Very High Resolution Radiometer (AVHRR) and Advanced Microwave Scanning Radiometer (AMSR) infrared and microwave sensor measurements and produces a global daily median SST and associated standard deviation (SD) as a measure of uncertainty associated with each pixel.

Validation of data was achieved through matching up the data to *in-situ* measurements taken by Met Éireann buoys along the South-West Coast of Ireland.

2.1 Study Area

An area was chosen within the North Atlantic, to include the four meteorological buoys M3, M4, M5 and M6 off the coast of Ireland, extending from 44.1250 to 55.1250 °N and from 5.8750 to 33.8750 °W (Fig. 2). According to the data specifications of the satellite data each pixel extends by 0.05 ° (Veal and Corlett, 2017; Merchant, et al., 2014a), hence the study are included 44 x 112 pixel, a total of 4'928 pixel.

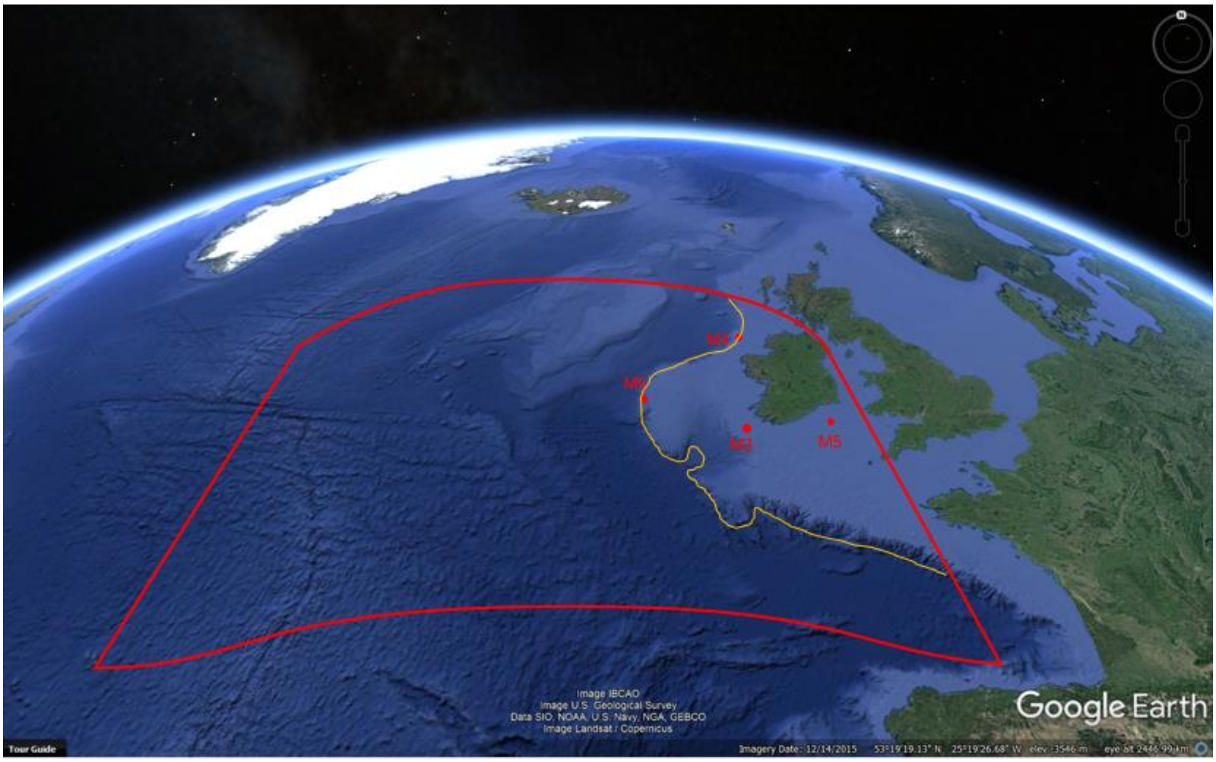

Fig. 2: Location of study area and Met Éireann Buoys M3, M4, M5 and M6. (source: Google Earth, 2017).

This Area of Interest (AOI) includes an extensive area of the Irish Continental Shelf, which is highlighted in Figure 2 by the orange line. The M6 buoy is located at the edge of the Porcupine Bank, which continues on to form the Porcupine Abyssal Plain, while the M4 buoy is located on the edge of the Rockall Trough (Marine Institute, 2018a). This marine biome is located in a mild climate and includes a diverse range of habitats, biodiversity and is considered of amenity value (Marine Institute, 2018b). The economic value of Ireland's oceans was found to add up to € 1.2 billion in the year 2010 (Marine Institute, 2018b). Marine resources include shipping, tourism, fishery and aquaculture activities, as well as oil and gas and renewable ocean energy resources (Marine Institute, 2018b).

2.2 Satellite sensor data

Satellite sensor data, in detail the ESA SST CCI GMPE Lv. 4 product, was acquired from the ESA SST CCI project through the Centre for Environmental Data Analysis (CEDA) (STFC, 2011c). The GMPE Lv. 4 product is a blended product of three ATSR infrared sensors, one AVHRR infrared sensor and one AMSR microwave sensor over the years from 1981 to 2016 (see Table 1 for details) in a daily 0.05 ° latitude by longitude grid (Veal and Corlett, 2017; Merchant, et al., 2014a), however, so far only data covering the period from 1981 to 2010 has been made available through CEDA. The three ATSR Level 1 sensors, ATSR-1, ATSR-2 and AATSR, are all in a sun-synchronous polar orbit, and hence pass over the same location at the same time every day. Merchant *et al*. (2014a) have specified this time to be 1030h and 2230h, expect for very high altitudes. The ATSR sensor observations provided the calibration reference for the other datasets (Merchant, *et al*., 2014a). The AVHRR-3 sensor was included into the data set in case of loss of the AATSR sensor and hence deliver an alternate reference. The AVHRR-3 sensor was operational from 2006 (Table 1). The microwave sensor, AMSR-E, was also in sun-synchronous polar orbit. The AVHRR sensor was the only non-sun-synchronous polar-orbiting sensor. In general, polar orbiting satellites can be of higher resolution than geostationary satellites due to their placement at lower altitudes.

Table 1: Satellite Data Access Requirements and Sensor specifications, SST CCI (source: Veal and Corlett, 2017).

Product name	Sensor(s)	Sensor type	Characteristics	Available temporal coverage
ATSR Level 1	**ATSR-1, ATSR-2, AATSR**	Visible and infra-red radiometer	Sun-synchronous polar orbits	1991 – 2012
AVHRR GLOBAL GAC L1	**AVHRR**	Visible and infra-red radiometer	Polar orbits	1981 – 2016
AVHRR FRAC Level 1 (included as alternate reference for AATSR)	**AVHRR-3**	Visible and infra-red radiometer	Sun-synchronous polar orbits	2006 – 2016
AMSR-E Level 1	**AMSR-E**	Microwave radiometer	Sun-synchronous polar orbits	2002 - 2012

Combined observations of all sensors mentioned above correspond to a SST at a depth of 20 cm (GHRSST, 2018; Merchant, *et al.*, 2014a; STFC, 2011a). In order to compute the temperature at 20cm depth, an estimate for the correction of the oceanic thermal skin layer and the vertical near surface thermal stratification is added to the SST_{skin} observation for each pixel (Merchant, *et al.*, 2014a). Because of the algorithm that is applied to correct for any known effects in the water column, this 20 cm depth measurement is expected to be free of diurnal effects (Merchant, *et al.*, 2014a). This explains further, why the CEDA and ESA CCI product specifications refer to the GMPE product measurement depth as an SST_{fnd} measurement, rather than an SST_{depth} measurement (see Figure 1), because a SST foundation measurement is considered to be free of diurnal variation. Measures of uncertainty are applied to the product in order to quantify the doubt associated with each measurement and are given in standard deviation (Merchant, *et al.*, 2014a); the standard error from the mean. Factors such as radiometric noise, instrumental noise, calibration errors and atmospheric variability are applied (Merchant, *et al.*, 2014a). Effects of radiation from the atmosphere due to scattering by aerosols and atmospheric water vapour are removed in the ATSRs through their dual view (Maurer, 2002).

SST in the GMPE product is provided as a gridded product at resolution of order 0.05 ° and the referencing system is set to WGS 84 (World Geodetic System) due to user requirements and to allow comparison with other products (Bulgin, *et al.*, 2016; Merchant, *et al.*, 2014a).

ATSRs and AVHRRs observations correspond to an SST_{skin} depth, whereas AMSRs observations correspond to an $SST_{sub\text{-}skin}$ depth (see Fig. 1). The AVHRRs allows for an easy correction of atmospheric effects, but are sensitive to surface roughness and precipitation (Maurer, 2002). Additionally, while the thermal IR is affected by cloud cover, the passive microwave lengths can penetrate cloud cover, enabling the CCI product to acquire a daily composite of SST, as opposed to the previous weekly and monthly composites.

The optimal interpolation that was applied to the product was an improved product from the OSTIA, which was first used on the AVHRR instrument and reanalysed each obtained SST measurements with the previous day's measurement in order to detect any errors or deviations. It was improved for the purposes of the SST CCI to allow for satellite-only input data and better capture the high resolution features of the data (Merchant, *et al*., 2014a). For the Level 3 product, *in-situ* observations are specified in detail in the Data Access Requirement Document, which was authored by the ESA SST CCI team members Veal and Corlett (2017), and included observations from drifting buoys, shipborne radiometers, the Global Tropical Moored Buoy Array and Voluntary Observing Ships (Veal and Corlett, 2017). According to the ESA SST CCI product specifications (Merchant *et al*., 2014a), ship and buoy data that was included in the reference data set, was quality controlled in line with the methods set out in Atkinson *et al*. (2013) and gridded using the methods set out in Rayner *et al*. (2006). Quality control was applied retrospectively in order to allow quality assessment over time. It was executed through "tracking" SST observations from drifting buoys and voluntary observing or research ships against the OSTIA SST_{fnd} values as a reference. Common gross errors in the drifting buoy data were flagged or ship call signs blacklisted in cases where the observations were "deemed unreliable" (Atkinson *et al*., 2013). The bias correction that was applied in these Level 3 *in-situ* data fields was used as a reference to improve the OSTIA product (Reynolds, *et al*., 2007; STFC, 2011c) and allow the Level 4 product to be independent of *in-situ* measurements (Merchant, *et al*., 2014a). Furthermore, correction for data gaps, occurring due to cloud cover or swath limitations, formed an important aspect of the optimal interpolation product (Good and Rayner, 2013; Merchant, *et al*., 2014a).

2.3 *In-situ* data

Fig. 3: Met Éireann ODAS buoy, part of the Irish Weather Buoy Network, operating from 2000 to 2011 (Met Éireann, 2016).

Four meteorological buoys from the Irish weather buoy network (see Fig. 3) were selected to provide the *in-situ* SST data. The Irish weather buoy network is managed by the Marine Institute in collaboration with Met Éireann, the Irish Meterological Service, and the UK Met Office (Marine Institute, 2018c). The buoys were selected because of their long-term continuous data reporting, quality controlled data and their geographic location. The inclusion of other moored buoys was considered, but due to the limitations of the study area, the four selected buoys were the only buoys available. Moored buoy are known to offer "accurate, near real-time, long-term and frequent observations from a fixed deep-water location" (Meindl, 1996).

Moreover, the addition of drifting buoys or measurements from voluntary or research ships was considered but rejected due to the complexity of matching-up data with the satellite sensor data or their non-continuous data recording.

The four selected buoys are moored to the Irish continental shelf; Figure 2 shows a map with the location of each buoy. The buoys closest to the Irish coast are the M3 and M5 buoy, located approximately 56 km southwest of Mizen Head and south of Hook Head. The M4 buoy is located approximately 83 km west of Rossan Point and the M6 buoy furthest away at approximately 390 km west southwest off Slyne Head (Met Éireann, 2018). Data was acquired for the 4 meteorological buoys, M3, M4, M5 and M6, from the Marine Institute archive for the years 2009 and 2010 (Marine Institute, 2018d). Buoy measurements were recorded and archived using 1 to 3 significant figures at real-time in 1-hour intervals, 24-hours a day since

2002 (M3 and M4), 2004 (M5) or 2006 (M6) respectively (Met Éireann, 2018). The buoys used are 2.8 metres in diameter (Meindl, 1996). Quality control was applied to the data, through the Marine Institute, retrospectively. An email (Alcorn, T., 2017, personal communication, 6 July) confirmed that the buoy measurements were taken at a depth of approximately 1 m.

Since buoy data had been used for the quality control of the satellite sensor data and hence ESAs own validation of the dataset, special attention was paid when selecting buoys for validation of the dataset in this study. Hence, records were searched for any evidence of the Met Éireann buoys being used for validation of the ESA dataset and personal correspondence with the project leader, Christian Merchant, carried out. He confirmed, that unless the buoys are broadcast on the Global Telecommunication System (GTS), they are not included in the validation process (Merchant, C., 2018, personal communication, 20 February). Moreover, as pointed out in Section 2.2., while the GMPE product was validated by in-situ data during the production stage, the final product was built to be independent of in-situ data (Merchant, *et al.*, 2014a).

2.4 Data processing

In Phase 1, the satellite dataset comprising of daily satellite images available in Network Common Data Form (.netCDF-4) was converted to .img-format. Within that, the SST variable had ancillary product quality data stored with it and the standard deviation (SD) associated with each pixel was extracted from that and equally converted to .img-format. All files were renamed with a nomenclature that included a time and date stamp and indication of SST or SD in order to allow data matchup with the buoy data at a later stage. Two geoprocessing software suites were used: Esri's ArcGIS geographic information system and the ERDAS Imagine (licence provided by UCCs Department of Geography) remote sensing application.

In Phase 2, the buoy data was processed using Microsoft Excel, to compute daily median values and interquartile ranges as a measure of uncertainty. Daily medians were computed by taking all the available measurements for each day, which were up to 24 measurements per day, sorting the measurements from lowest to highest value and assorting the middle value (2nd quartile, below which 50% of the values lie) as the median. The 1st and 3rd quartile (below which 25% and 75% of the values lie) were then assigned in order to compute the interquartile (Q3 - Q1 = IQR) range. The buoy data had been recorded between 1 and 3 significant figures and was only reduced at the end of the calculations, to between 3 and 4 significant figures (2 decimal places), in order to minimise errors. Data gaps were accounted for, as not every day included 24 measurements. The buoy data was then divided into data cubes to include only one measurement every 5 days.

In Phase 3, the data processing was undertaken to allow comparison of the satellite sensor and buoy data. Images were subset to the area of interest (AOI) and clipped using the ERDAS Imagine software in a batch process. In the next processing step, a model was built in order to batch process the SST dataset and the SD dataset. A land mask was extracted using ArcGIS and applied in ERDAS Imagine to remove all values corresponding to land cover from the island of Ireland (Steps 3.1 and 3.2 in Fig. 4). As part of the processing, the data was divided into data cubes, which included only one image every 5 days within the two year period covering 2009 and 2010. This was done for the SST variable and the SD variable (Steps 3.3 and 3.4 in Fig. 4). Following that, a layer stack was carried out for the SST and SD data cubes separately (Step 3.5), in preparation for the next step, the point extractions. A shape file from the Marine Irish Digital Atlas (MIDA, 2015) was downloaded, containing buoys from the Irish Marine Data Buoy Network and the UK's Marine Automatic Weather Stations (MAWS) network, and a separate layer created to include only the M3, M4, M5 and M6 buoys, using ArcGIS (Step 3.6). Special attention to the geographic location of the buoys was paid in order to allow a matchup of the data as precisely as possible.

Point extractions were then carried out for the SST and the SD variable using the ArcGIS's geoprocessing tool "Extract Multi Values to Points" in order to only consider the pixels that include the buoy location values for the M3, M4, M5 and M6 buoys in the analysis. Point extraction values were extracted from the images in a table format and formatted using Microsoft Excel (Steps 3.7 and 3.8). The SST and SD data was then converted from units Kelvin to degrees Celsius. In the next step, the point extraction SST values from the satellite images were matched up and compared with the SST values computed from the buoy datasets using Microsoft Excel and the calculated IQR applied to the buoy measurements and the point extracted SD applied to the satellite sensor measurements (Step 3.9.1). Analysis of these will follow in the results section of this paper.

The last data analysis step consisted of using IBM's statistical analysis software SPSS in order to conduct a regression analysis using scatter-plots (Step 3.9.2). The matchup data was imported as numeric type variables from the Microsoft Excel spreadsheet and scatter plots conducted using between 3 and 4 significant figures, depending on the data. All data processing steps are summarised in Figure 4.

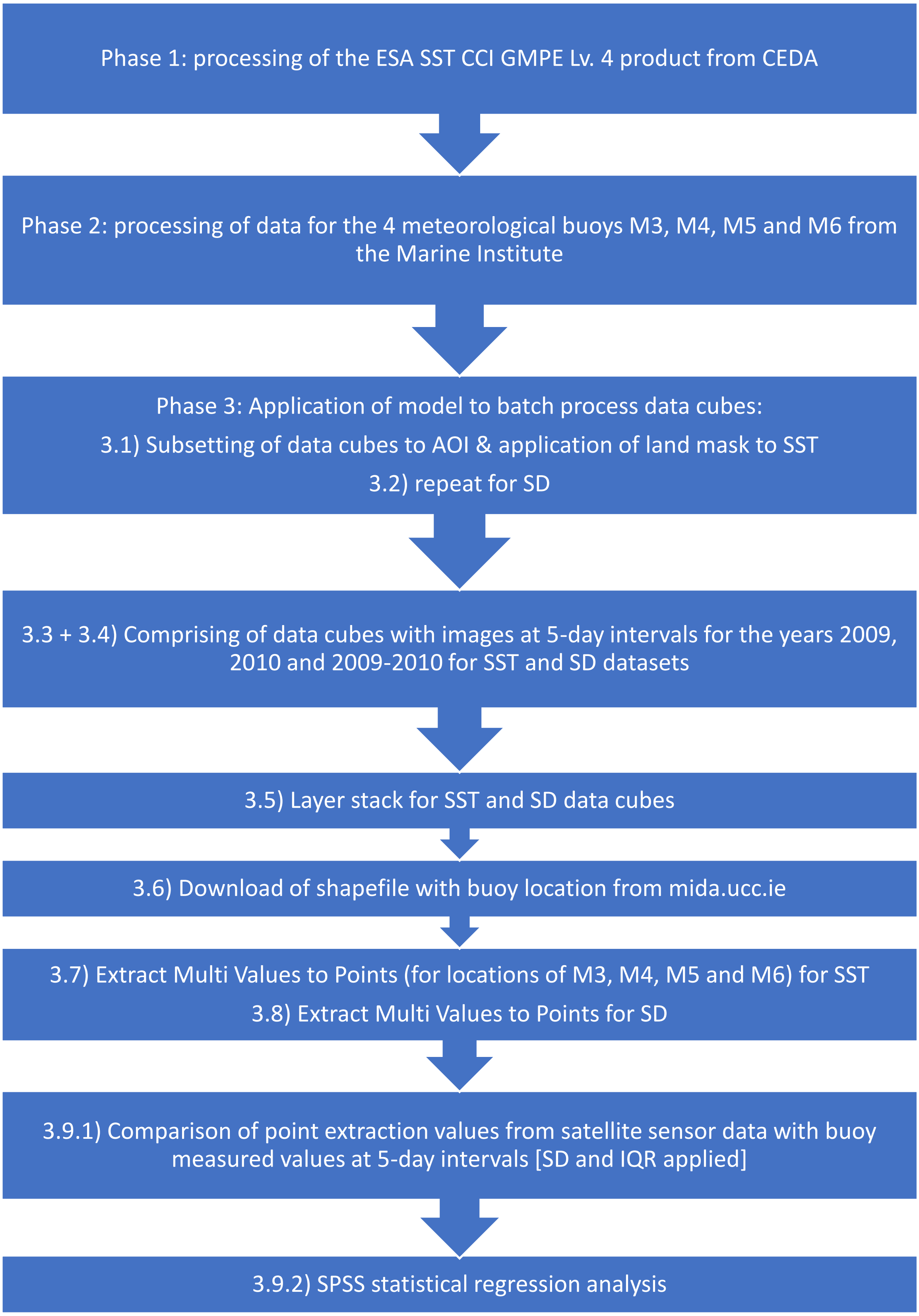

Fig. 4: Schematic of data processing steps from Phase 1: processing of the satellite data, Phase 2: processing of the buoy data to Phase 3: processing of the match-up data.

3. Results

A matchup of the buoy data and the satellite sensor data was carried out in order to assess the accuracy of the ESA SST CCI dataset. Descriptive, qualitative, quantitative and exploratory data analysis methods were used. The descriptive analysis of medians, standard deviations and interquartile ranges examined the features of the data in preparation for the quantitative analysis. Median SST measurements obtained by the satellite sensors ranged from 7.61 to 16.67 °C, those obtained by the buoys ranged from 7.4 to 18.00 °C, hence measurements obtained by the satellite sensors were overall colder. The standard deviation, as a measure of uncertainty associated with the satellite sensor data, ranged between 0.1 and 0.87 °C. Interquartile range, as a measure of the uncertainty associated with the buoy measurements, differed between 0 and 1.15 °C, indicating large variability within the buoy data. Qualitative analysis of the data aimed to highlight any patterns in the data. Figure 5 shows the median SST trends for each of the 4 buoy locations over the period from 01.01.2009 to 31.12.2010 at 5-day intervals, measured at a depth of approximately 1 m. The general pattern, with a cooling trend in winter and warming trend in summer could be observed for each of the 4 buoy locations. However, their location at different latitudes reflected in the data; the M4 buoy, being located at the highest altitude, showed the overall coolest SST, while one anomalous peak value was observed in summer 2009. The M6 buoy trend showed the lowest variance; it is also the buoy located at the furthest distance from the island of Ireland. The M5 buoy showed the highest variability from winter to summer and the M3 buoy followed a similar trend as the M4 buoy, though SST measurements were slightly warmer. As part of the quantitative and exploratory analysis, the time-series, deviations and correlations were computed in order to examine any relationships. Figures 6 a-d show the median SST trends for each of the 4 buoy locations over the period from 01.01.2009 to 31.12.2010 at 5-day intervals as measured by the satellite at 20cm depth and the buoys at approximately 1 m depth. Deviations are indicated either by the standard deviation, for the satellite sensor data, or by the interquartile range, for the buoy data. It was observed that the satellite sensor and the buoy data followed a similar trend and showed a seasonal cooling trend in winter and spring and a seasonal warming trend in summer, with the exception of the year 2010, where a seasonal warming trend persisted into autumn (see Figs. 6 a-d). To examine correlations, inferential statistics were applied and a regression analysis carried out through producing scatter plots (see Figs. 7 a-d).

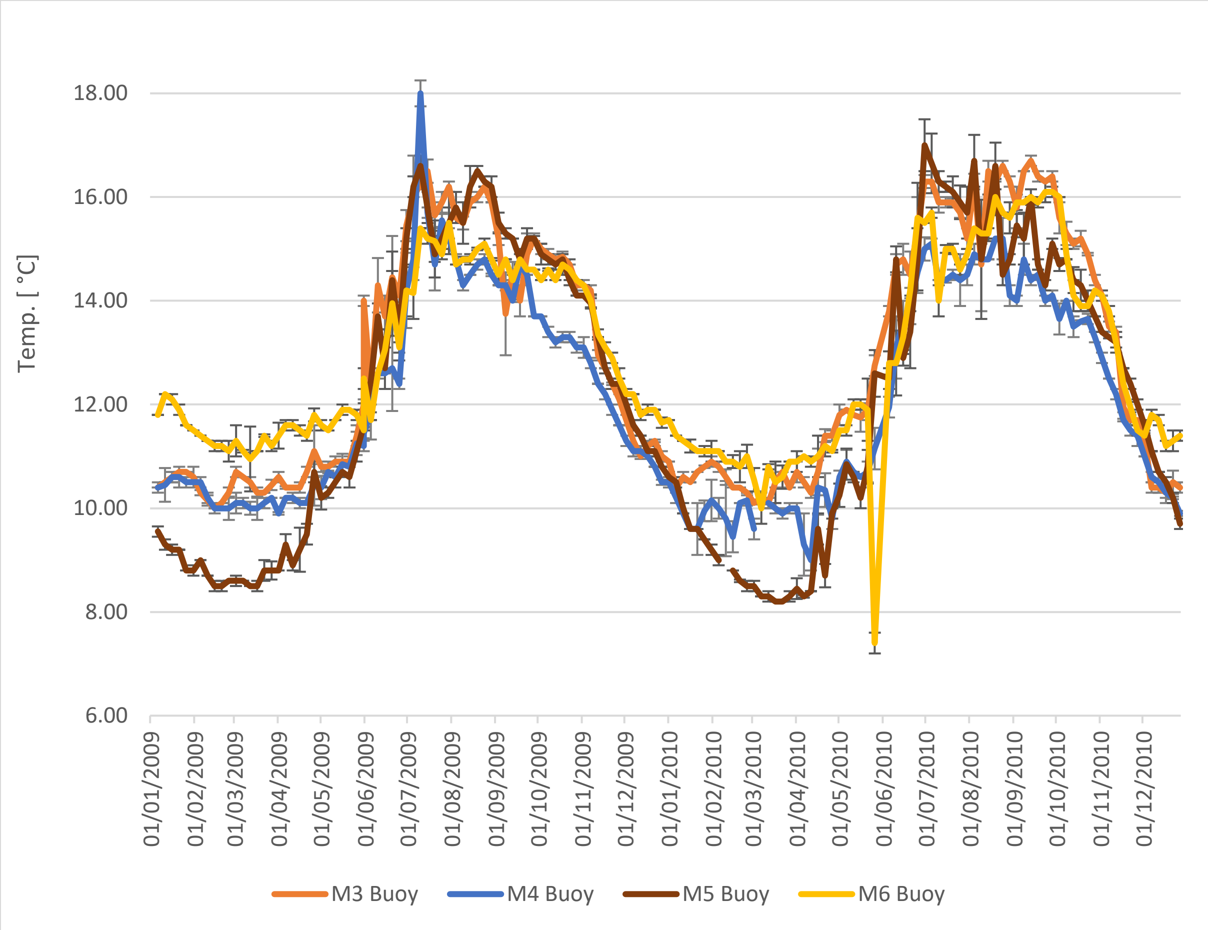

Fig. 5: Median sea surface temperature for the four Met Éireann buoys from 01.01.2009 to 31.12.2010 at 5-day intervals as measured at approximately 1 m depth [IQR as a measure of uncertainty].

It was found that the satellite sensor data matched the M3 buoy (Fig. 6a), at location 51.2166 °N, 10.5500 °W, general trend, with an average deviation of 0.18 °C. A maximum deviation from the satellite sensor data occurred on the 3rd of September 2009, when the recorded buoy data was 1.18 °C lower than the satellite sensor data. A second large deviation occurred 10 days later on the 13th of September 2009, when the buoy data recorded a SST 1.10 °C lower than the satellite sensor data. The buoy data for these two days was found to have a large uncertainty associated with it [IQR] (Fig. 6a). The scatter plot showed, that a strong positive linear relationship (R^2= 0.99) between the satellite sensor data (dependent variable) and the buoy data (independent variable) existed (Fig. 7a). In detail that meant, that 99% of the variation was determined by the regression line and 1% by some other factors. Three outliers were identified and associated with a warm bias in the satellite sensor data.

Buoy M4 (Fig. 6b), at location 54.9982 °N, 09.9922 °W, was the buoy that overall showed the largest deviations from the satellite sensor data, with an average deviation of 0.85 °C and a maximum deviation of 7.84 °C on the 2nd of March 2010. This deviation could be traced back to data gaps and hence a second large deviation was identified and found to have deviated 2.54 °C on the 20th of February 2010. It was found that, when comparing the satellite sensor and buoy data, the M4 buoy underestimated SST in summer and autumn and overestimated SST in winter and spring. The scatter plot for the M4 data matchup (Fig. 7b) showed a strong positive linear relationship ($R^2 = 0.937$). One outlier was identified and associated with a warm bias in the buoy data.

The M5 and M6 buoys, similar to the M3 buoy, were found to follow the satellite sensor data in their general trend and deviations were small. The M5 buoy (Fig. 6c), located at 51.6900 °N, 06.7040 °W, showed an average deviation of 0.28 °C. A maximum deviation was identified for the 5th of February 2010, with the highest deviation that was found in the whole data set, showing a measurement of 9.17 °C. This deviation was traced back to data gaps and hence a second large, but significantly smaller deviation was identified for the 30th of July 2010, with a deviation of 1.51 °C between the buoy and satellite sensor SST measurement. The scatter plot (Fig. 7c) showed a strong positive linear relationship ($R^2 = 0.988$). Two outliers were identified and associated with a warm bias in the satellite sensor data.

The M6 buoy (Fig. 6d), located at 53.0748 °N, 15.8814 °W, showed an average deviation of 0.22 °C and a maximum deviation with 4.75 °C difference in SST for the 21st of May 2010. This deviation was identified to be an abnormality within the buoy data associated with a 3-day period in which the M6 buoy recorded unusually low temperatures. The scatter plot for (Fig. 7d) showed a strong positive linear relationship ($R^2 = 0.936$), but the lowest overall. One outlier was identified and associated with a cold bias in the buoy data. Overall, the scatter plots indicated that annually, the M3 and M6 buoys are located in overall warmer water (between 10 and 16 °C) and the M4 and M5 buoys are located in overall colder waters (between 8 and 16 °C).

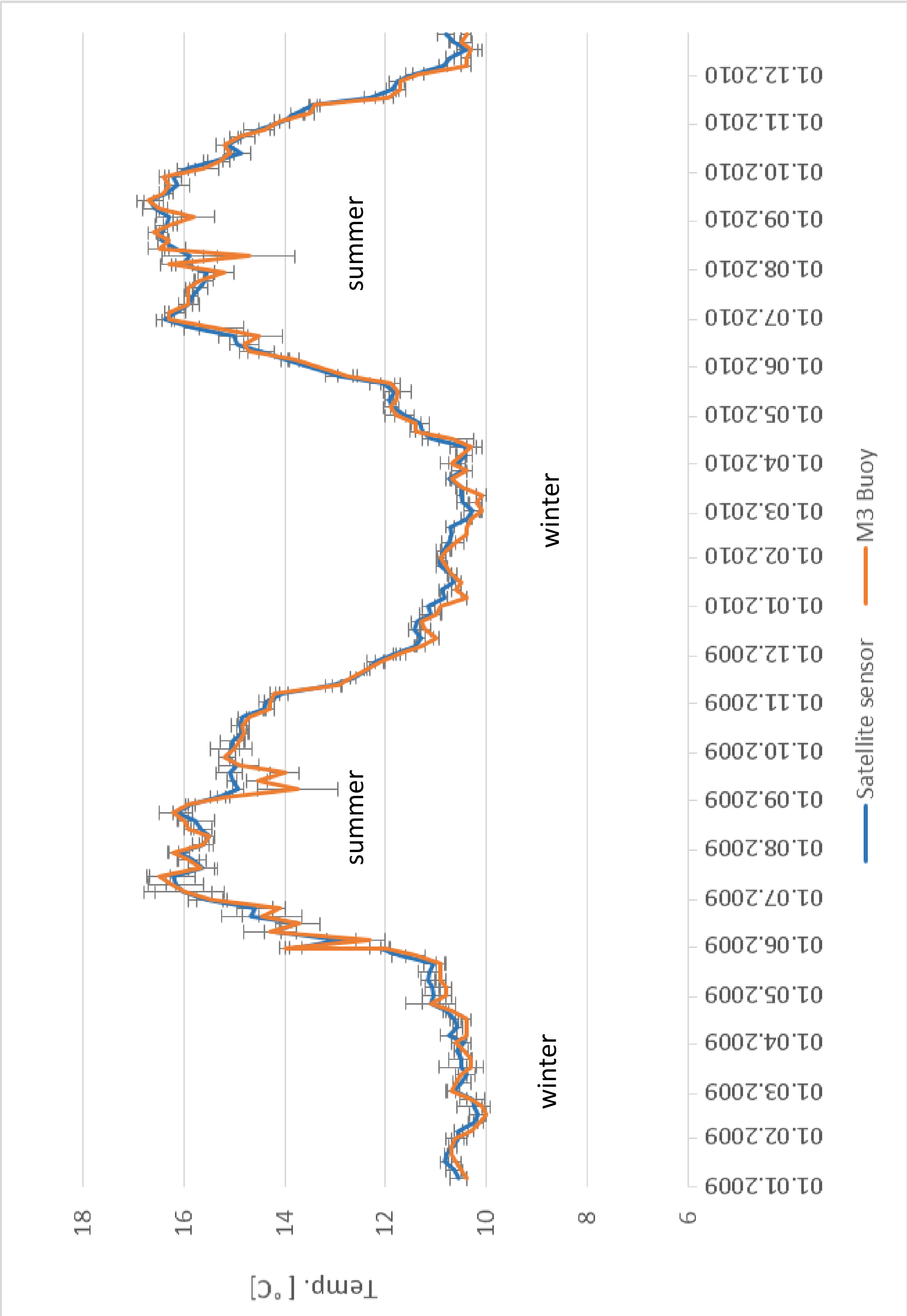

Fig. 6a: Median sea surface temperature at the location of the M3 buoy (51.2166 °N, 10.5500 °W) from 01.01.2009 to 31.12.2010 at 5-day intervals as measured by the M3 Buoy at approximately 1 m depth [IQR as a measure of uncertainty] and the satellite at 20 cm depth [SD as measure of uncertainty].

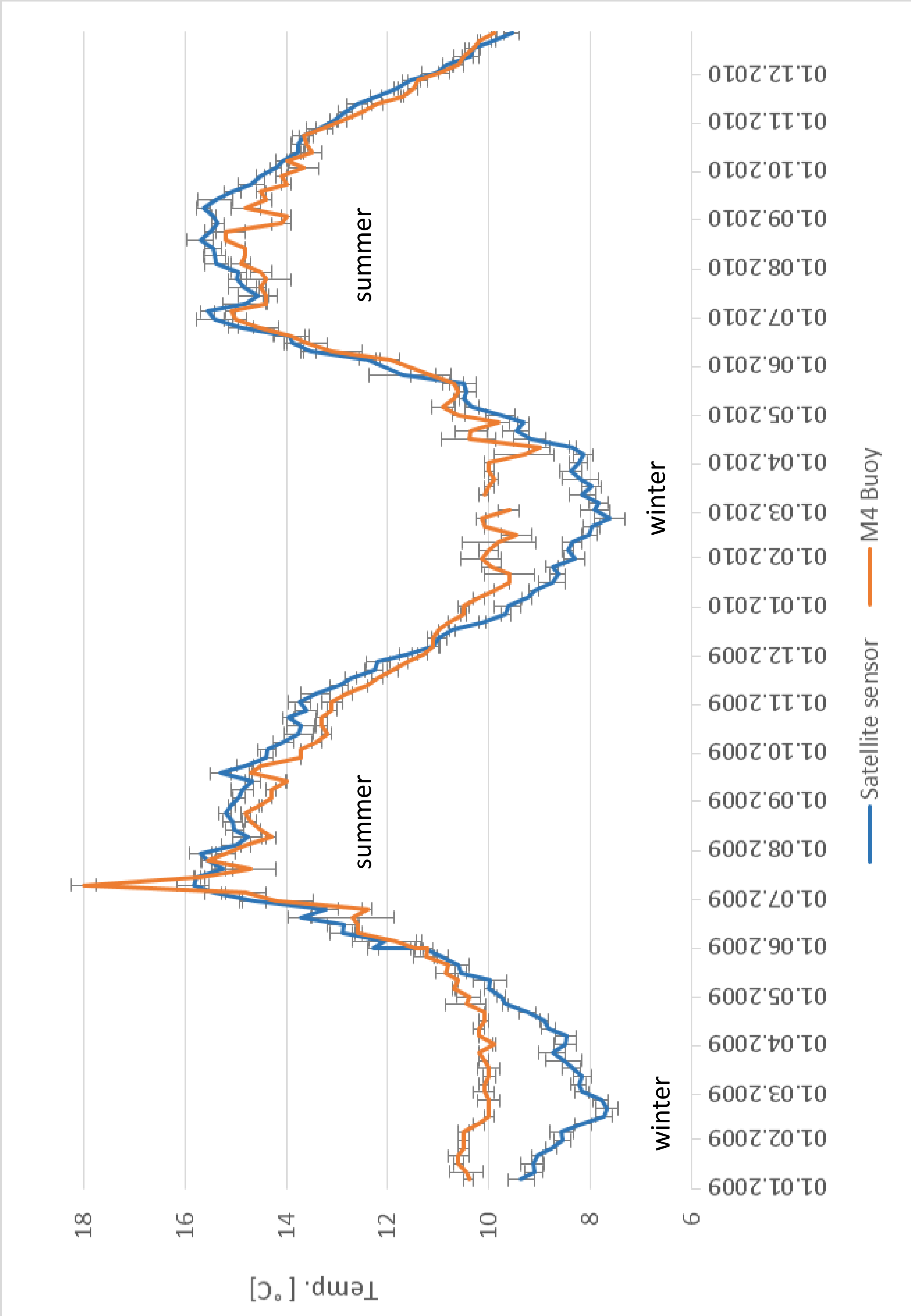

Fig. 6b: Median sea surface temperature at the location of the M4 buoy (54.9982 °N, 09.9922 °W) from 01.01.2009 to 31.12.2010 at 5-day intervals as measured by the M4 Buoy at approximately 1 m depth [IQR as measure of uncertainty] and the satellite at 20 cm depth [SD as measure of uncertainty].

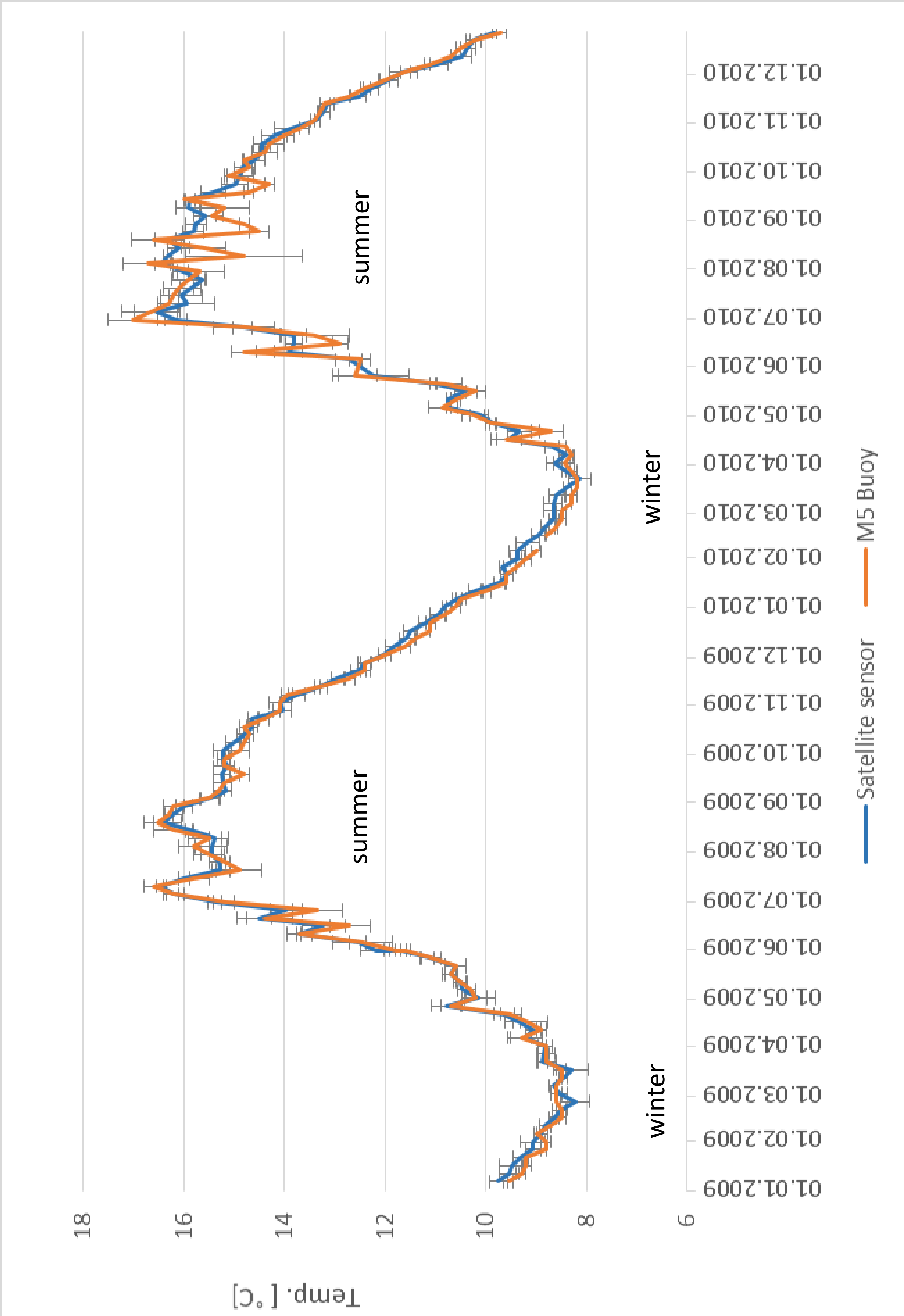

Fig. 6c: Median sea surface temperature at the location of the M5 buoy (51.6900 °N, 06.7040 °W) from 01.01.2009 to 31.12.2010 at 5-day intervals as measured by the M5 Buoy at approximately 1 m depth [IQR as a measure of uncertainty] and the satellite at 20 cm depth [SD as measure of uncertainty].

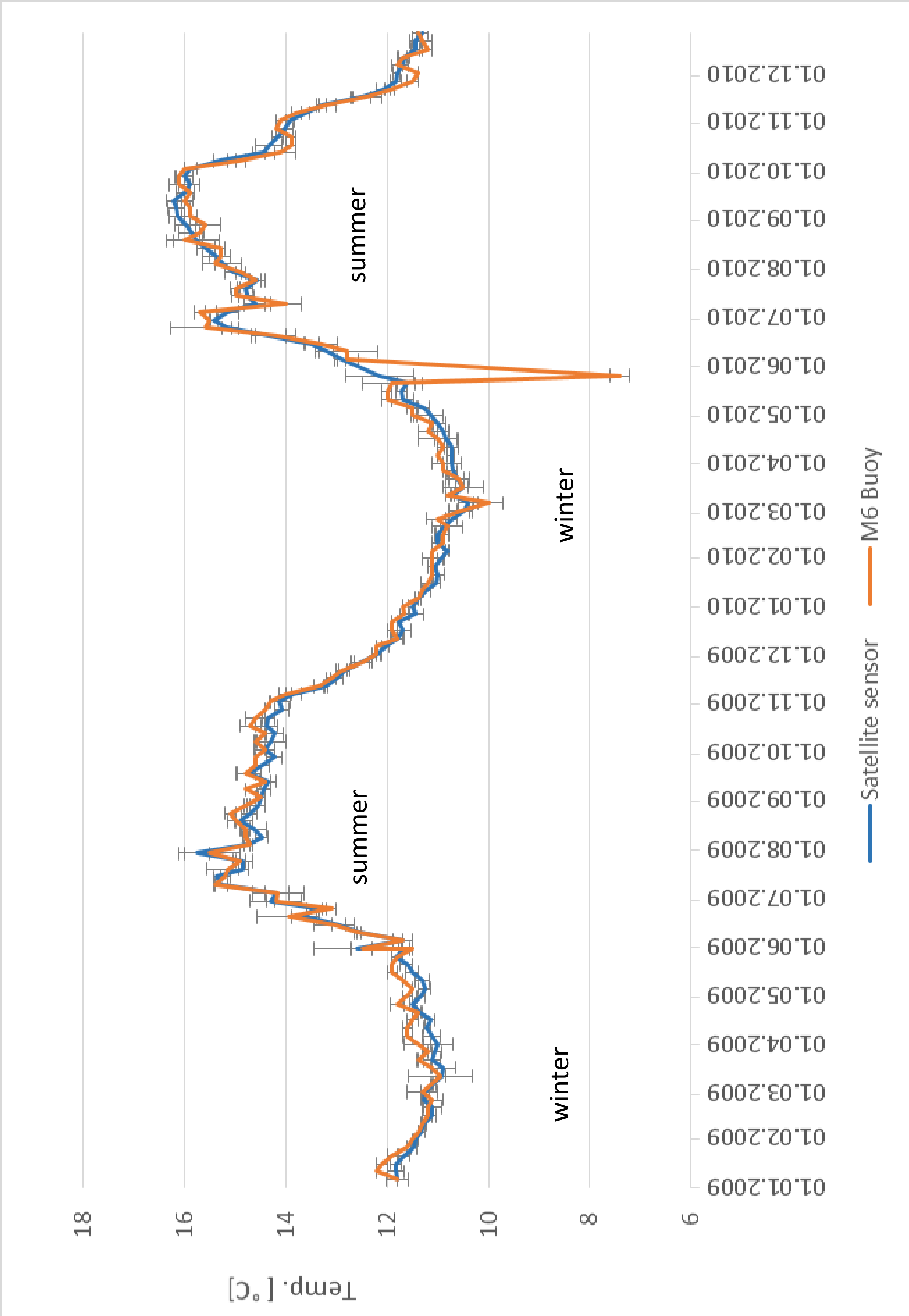

Fig. 6d: Median sea surface temperature at the location of the M6 buoy (53.0748 °N, 15.8814 °W) from 01.01.2009 to 31.12.2010 at 5-day intervals as measured by the M6 Buoy at approximately 1 m depth [IQR as a measure of uncertainty] and the satellite at 20 cm depth [SD as measure of uncertainty].

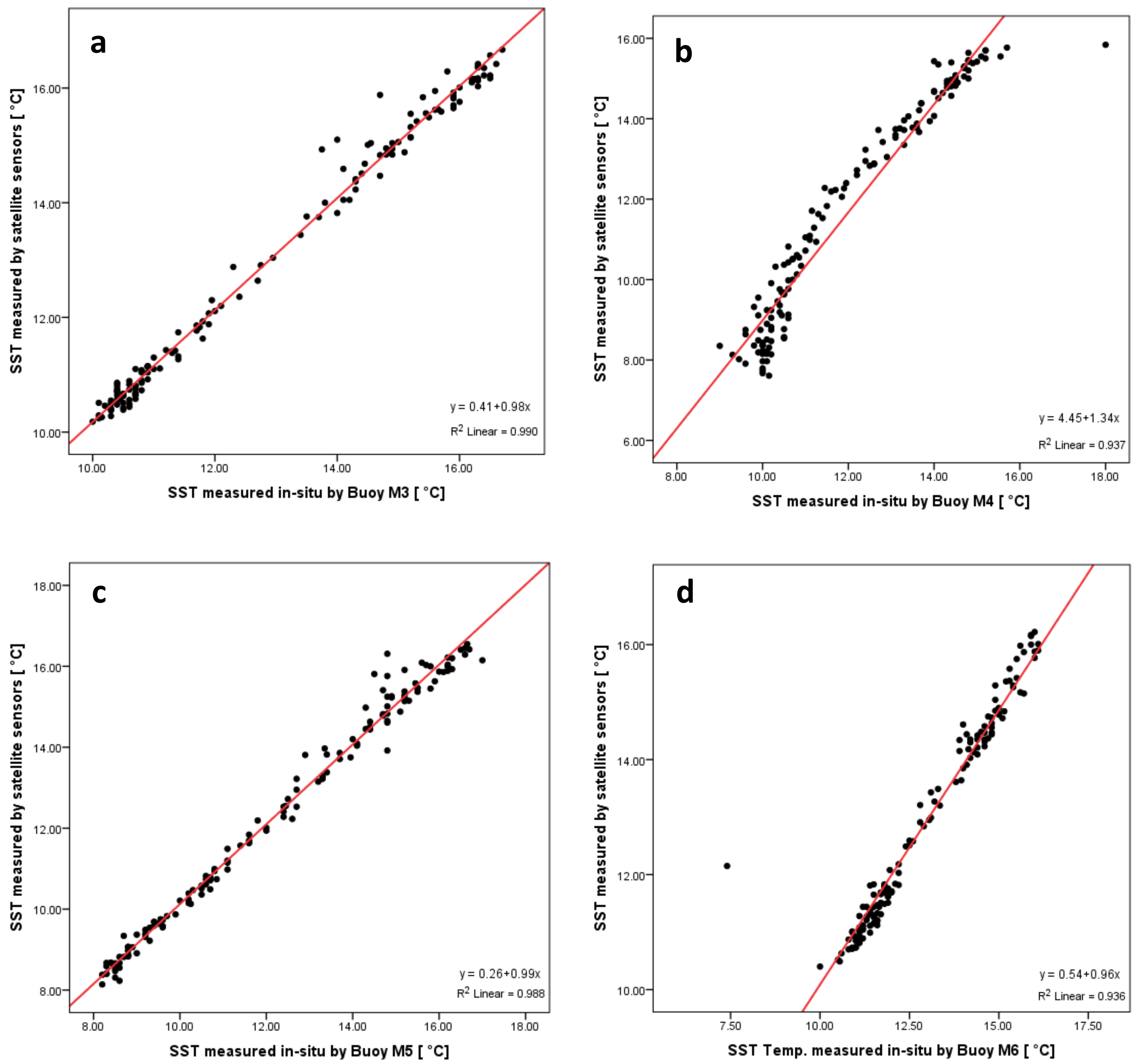

Fig. 7 a-d: Scatter plot of the satellite sensor and buoy SST data at the location of the (a) M3 buoy (51.2166 °N, 10.5500 °W), (b) M4 buoy (54.9982 °N, 09.9922 °W), (c) M5 buoy (51.6900 °N, 06.7040 °W) and (d) M6 buoy (53.0748 °N, 15.8814 °W) in the period from 01.01.2009 to 31.12.2010 at 5-day intervals [°C].

The deviations between the buoy and satellite sensor SST data mentioned previously are further illustrated by Figure 8. The level of significance was set out to be at 0.1 °C (0.1 degrees Kelvin), but due to the amount of deviations, a second level of significance was set at 0.4 °C (0.4 degrees Kelvin) (see Fig. 9 for the significance levels). Although the M5 and M6 buoys show peak values in deviations, overall, the M4 buoy showed the highest average deviation (0.85 °C) and the highest number of significant deviations overall. In detail, for the M4 buoy, 105 measurements (out of a total of 146) were equal to or above 0.4 °C, which was more than six times the amount of measurements above the significance level of 0.4 °C that were detected for buoys M3, M5 and M6 (see Table 2). Measurements for these buoys that were equal to or above 0.4 °C accumulated to a count of 14, 16 and 10 respectively. In turn that showed that out of the 146 total measurements observed, 132, 130 and 136 measurements out of 146 were below the 0.4 °C significance level. The trends observed for the 0.1 °C significance level were the similar, with the M4 buoy showing the highest number (136) of significant deviations (Table 2). Significant counts below the 0.1 °C level were between 54, 10, 48 and 45 for the M3, M4, M5 and M6 buoy locations (Table 2).

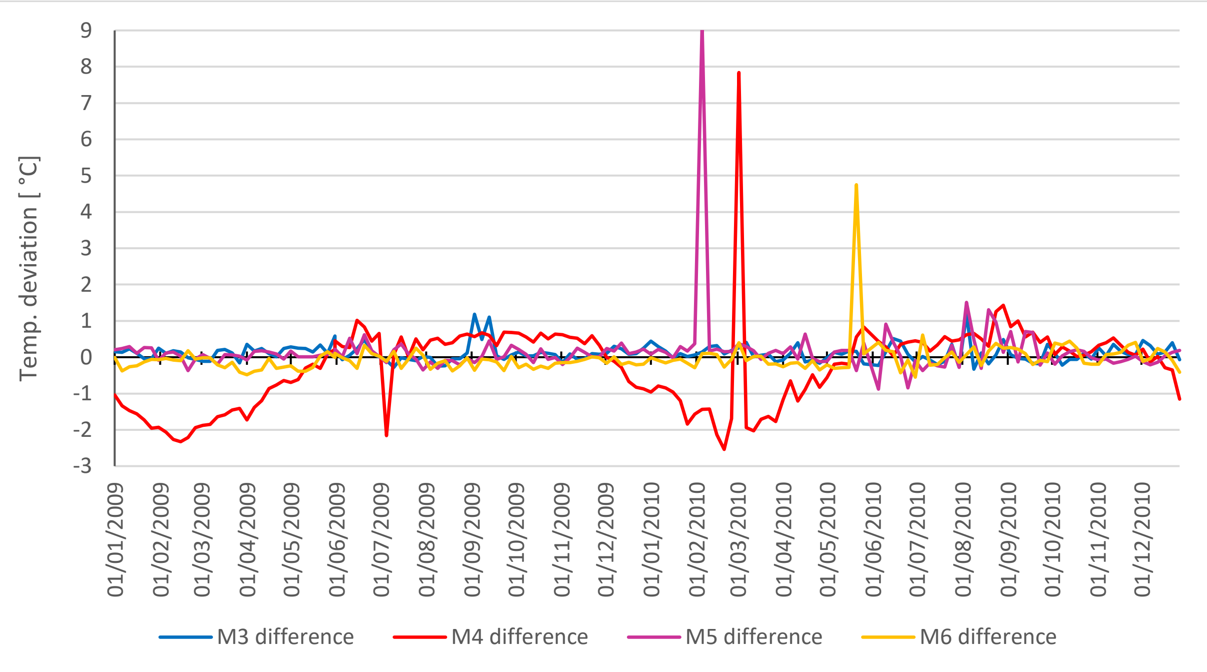

Fig. 8: Deviations between the satellite and buoy measurements of SST for each of the 4 buoy locations at 5-day intervals over the period from 01.01.2009 to 31.12.2010.

Table 2: Total counts of deviations between satellite sensor and buoy measurements from significance level of 0.4 °C and 0.1 °C.

	Counts below 0.4 °C	Counts above or equal to 0.4 °C	Counts below 0.1 °C	Counts above or equal to 0.1 °C
Matchup location of M3 buoy	**132**	14	54	92
Matchup location of M4 buoy	41	**105**	10	**136**
Matchup location of M5 buoy	**130**	16	48	98
Matchup location of M6 buoy	**136**	10	45	101

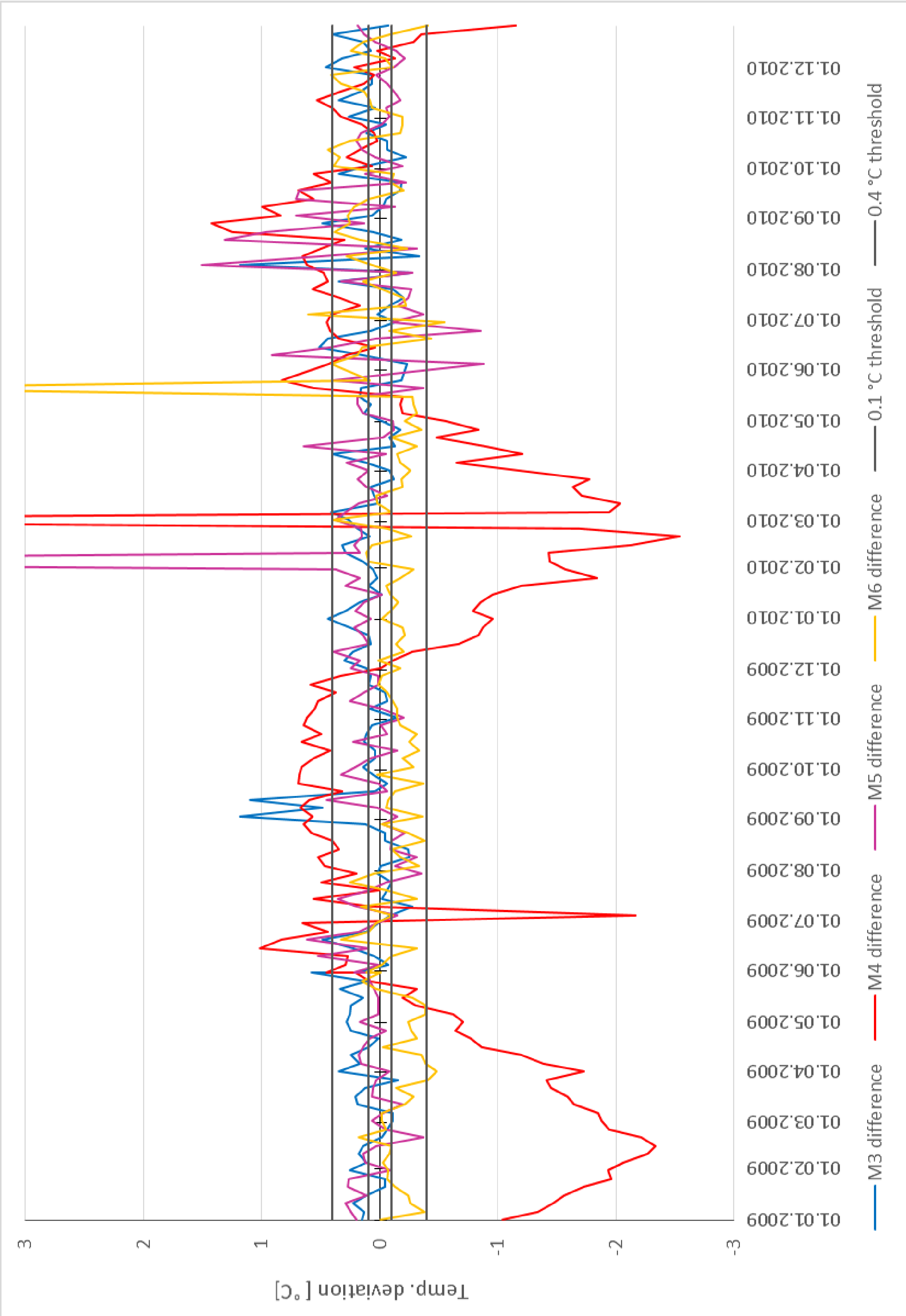

Fig. 9: Deviations on a scale from 0 to 3°C between the satellite and buoy measurements of SST for each of the 4 buoy locations at 5-day intervals over the period from 01.01.2009 to 31.12.2010.

One step further, within the regression analysis, residual diagnostics were carried out (Figs. 10 a-d). While the regression analysis examined and modelled the relationship between the satellite sensor and the buoy SST measurements, the residuals show the difference between the observed and predicted buoy temperature. For each of the four match-up locations, the buoy SST measurements for the whole time-series were correlated with the satellite sensor SST measurements. The buoy data was taken as the dependent variable and the satellite sensor data as the independent variable. Residuals were plotted with the standardized predicted values on the x-axis, indicating the prediction of the model, and the standardised residuals on the y-axis, indicating the accuracy of the prediction. A LOESS (Locally Weighted Scatterplot Smoother) curve was applied to show the non-linear best fit. Q-Q-plots, associated with each residual diagnostic, indicate if the residuals were normally distributed.

The residual diagnostics for the M3 buoy location (Fig. 10a) shows heteroscedasticity; the residuals increase as the predicted values increase. The data is skewed towards low standardized residual values, indicating that the model prediction overestimated these values. The Q-Q-plot indicated, that the residuals were near normally distributed and showed three outliers. Similar results were found for the M5 buoy location (Fig. 10c), where the data indicates heteroscedasticity; as the residuals get larger, the prediction moved from small to large. The associated Q-Q-plot indicated a near normal distribution and showed six outliers. The residual diagnostics for the M4 buoy location highlight nonlinearity between the standardized residuals and the predicted values (Fig. 10b). The prediction was too high for high (+1) and low (-1) predicted values and the prediction was too low for predicted values around zero. The Q-Q-plot showed a near normal distribution and one outlier. The residual diagnostics for the M6 buoy location (Fig. 10d) showed a Y-axis unbalance, caused by large impacts of outliers. The scatterplot shows one large outlier, while the Q-Q-plot indicates that the data is not normally distributed, hence supporting the finding of a skew in the scatterplot data.

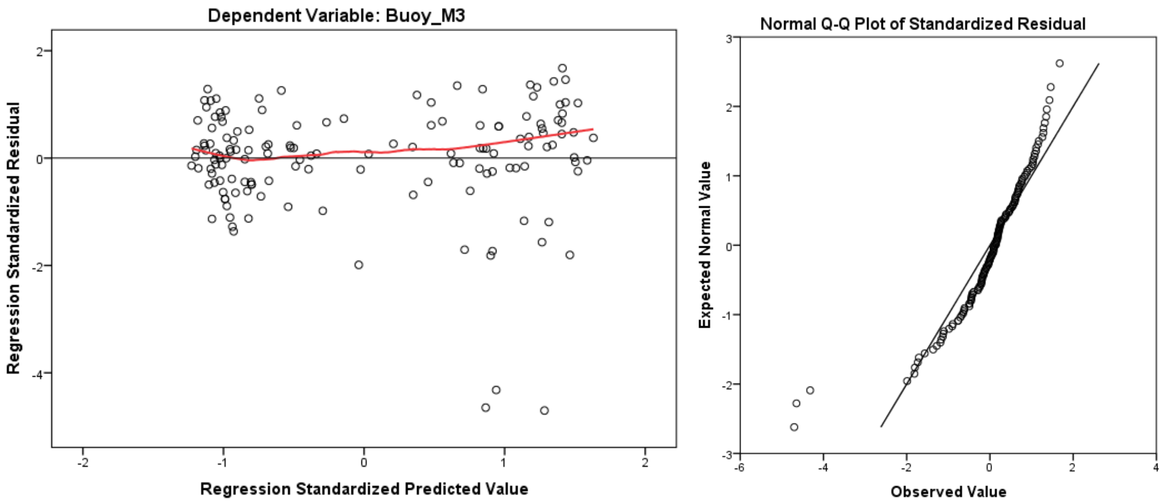

Fig. 10a: : Residual diagnostics and Q-Q-plot for the satellite sensor and buoy SST data at the location of the M3 buoy (51.2166 °N, 10.5500 °W) in the period from 01.01.2009 to 31.12.2010 at 5-day intervals.

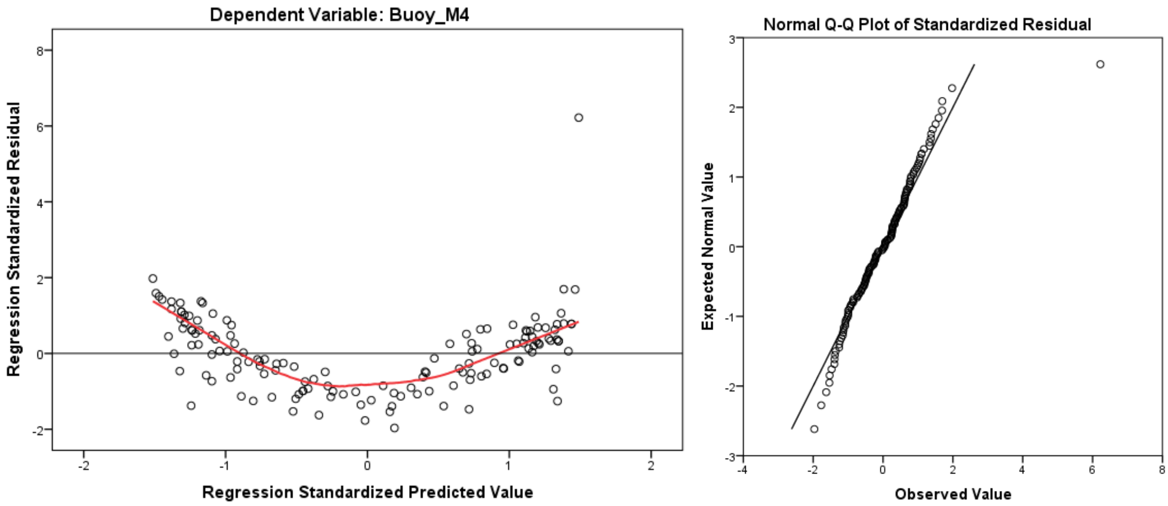

Fig. 10b: : Residual diagnostics and Q-Q-plot for the satellite sensor and buoy SST data at the location of the M4 buoy (54.9982 °N, 09.9922 °W) in the period from 01.01.2009 to 31.12.2010 at 5-day intervals.

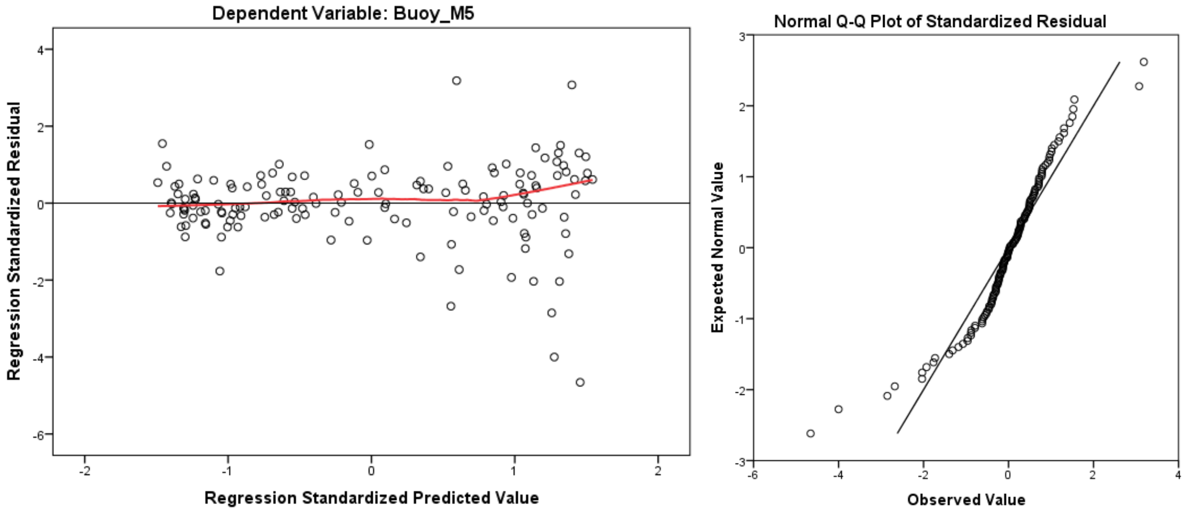

Fig. 10c: : Residual diagnostics and Q-Q-plot for the satellite sensor and buoy SST data at the location of the M5 buoy (51.6900 °N, 06.7040 °W) in the period from 01.01.2009 to 31.12.2010 at 5-day intervals.

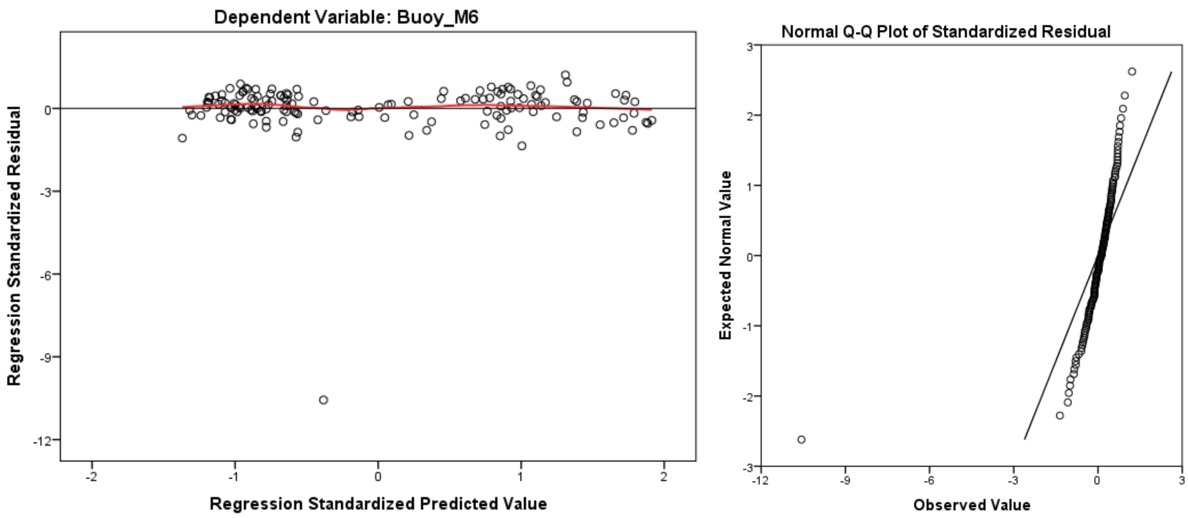

Fig. 10d: : Residual diagnostics and Q-Q-plot for the satellite sensor and buoy SST data at the location of the M6 buoy (53.0748 °N, 15.8814 °W) in the period from 01.01.2009 to 31.12.2010 at 5-day intervals.

While the aim of the Global Ocean Data Assimilation Experiment (GODAE), out of which the ESA SST Climate Change Initiative (CCI) progressed, was to produce a long-term data set of SST with an improved accuracy from 0.4 °C (0.4 K) down to 0.1 °C (0.1 K) (Donlon, *et al*., 2007), it was identified that none of the 4 tested buoys verified the accuracy of the data set within 0.1 °C (0.1 K). However, analysis of the deviations of each buoy has shown, that on average the M3 buoy could verify the satellite data within 0.18 °C, the M4 buoy within 0.85 °C, the M5 buoy within 0.28 °C and the M6 buoy within 0.22 °C. While this may not result in an accuracy improvement within 0.1 °C (0.1 K), this study was able to validate the accuracy of the satellite data accuracy within 0.18 and 0.28 °C, only considering buoys M3, M5 and M6 and hence able to validate data accuracy below the 0.4 °C threshold for these buoys. The M4 buoy however was above the 0.4 °C threshold, with a data accuracy of 0.85 °C.

4. Discussion

Overall, the assessment showed that the satellite sensor data for the North Atlantic region (for the observed AOI) could be reliably validated to within 0.18 °C for the M3 buoy location, 0.22 °C for the M6 buoy location, 0.28 °C for the M5 buoy location and 0.85 °C for the M4 buoy location. Natural variations, such as seasonal changes, could be observed. The data match-up showed strong positive linear correlations for all four match-up points. However, a few outliers have been identified and found to be associated with uncertainty (M3 buoy), data gaps (M4 and M5 buoy) and a 3-day period in which unusually low temperatures were recorded (M6 buoy), for which it was unable to establish the precise cause, but a calibration error was assumed. Moreover, the residual diagnostics showed heteroscedasticity in the M3 and M5 buoy data, indicating unequal variability and significant changes in the dependent variable from the beginning to the end of the time series. While this was not evident from the time-series analysis shown in Figs. 4a and c, the residual analysis indicated, that there was a large range between the smallest and largest values in the data, hence causing heteroscedasticity. Of particular interest here was, that the model over predicted for low standardised residual values, indicating that the satellite sensor data at the M3 and M5 buoy locations is less reliable in winter. Nonlinearity was detected for the M4 buoy location data, which fitted with previous findings of large deviations between the satellite sensor and buoy data. Moreover, the u-shape of the standardised residuals fit in with the previously detected seasonality error associated with the M4 buoy to underestimate SST in summer and overestimate SST in winter; the residual diagnostics indicated overestimation of high and low values. Lastly, the M6 buoy location showed a y-axis unbalance caused by outliers. This again was not evident from the time-series analysis (Fig. 4d), but highlighted by the Q-Q-plot and residual analysis (Fig. 10d). This result may be significant as it could potentially be traced back to a calibration error of the buoy or satellite.

Within this research, the question was raised, whether the Met Eireann buoys are currently used for validation of the ESA SST CCI data and hence cause a bias in the results. While this is of great concern, the evidence found in this study points to the buoys not being included. Particularly the results of the M4 buoy highlight, that if the buoys had been used for validation of the satellite sensor data, such a large discrepancy as was observed between the recorded satellite sensor data and the M4 buoy data should not have occurred. The M4 buoy was found to have the overall lowest count of match-ups with the satellite sensor data. As was highlighted in Table 1, only 41 out of 146 measurements matched up within a 0.4 °C threshold, while the other buoys matched up between 130 and 136 times. At the time of submitting this thesis, clarity from the Marine Institute was still awaited, on whether the M4 buoy malfunctioned or needed re-calibration in the years 2009 and 2010, as this may have significantly impacted the results.

The continuous findings of potential calibration errors within the buoy data in this study is a significant problem, as the buoy data was used as the "true" value of SST measurement in order to validate the satellite sensor data accuracy. However, sensor systems, such as those installed on the Met Éireann buoys, are known to have time variance associated with stratification, wave action, storm events and due to recalibration or malfunction. Over long-term buoys are known to be affected by salt water corrosion and biofouling and hence need maintenance every four to six years, recalibration every two to four years, while batteries last between three and four years (Meindl, 1996). Data on the specifics of the quality control measures used by Met Éireann is limited, but it was assumed that reliable, good-quality data was produced. This aspects need to be kept in mind when assessing the significance of the results. Homogeneity issues are not only known to affect *in-situ* instruments, it is also a long recognised issue in the satellite data record, when matching up different satellite instruments. Due to each instrument applying its own algorithm to correct for atmospheric and instrument bias, as well as different times the satellites are launched at and hence different rates of degradation of the instruments, ensuring homogeneity is quite complex. However, it is required in order to establish a reliable climate data record (CDR) for climate monitoring (Merchant, *et al*., 2014a; Posselt, *et al*., 2011). The study of Posselt *et al*. (2011) has shown, that even through the use of a self-calibration algorithm, the spectral difference of the observation between two sensors could not be corrected for. This application, which tried to correct for homogeneity bias when measuring solar surface irradiance, further highlighted, that other methods have to be examined in order to correct for the technological and spectral differences of the different satellite instruments. The importance of homogeneity and stability of time-series was highlighted by Merchant, *et al*. (2014a) and formed an important aspect of the satellite data that was examined in this study. Satellite data is known to be affected by clouds and aerosols present in the environment and be subject to technical issues such as sensor and satellite drift and homogeneity issues (Brinckmann, *et al*., 2014; Posselt, *et al*., 2011). When comparing and combining data from different platforms and sensors, special attention has to be paid to the depth at which the measurements were taken and also to related effects of diurnal heating, particularly during the afternoon, and evaporative cooling, which removes latent heat from the surface of evaporation. Several sensors, such as the Heliosat, have a self-calibrated algorithm to correct for degradation of satellite instruments over time and their discontinuities caused by replacement of satellite instruments (Posselt, *et al*., 2011). The optimal interpolation as well as the standard deviation that were applied to the GMPE product state to have covered all potential sources of error mentioned above. It is however questioned, how accurate the optimal interpolation estimates are. The OI for SST is a product that has been used and improved for decades of data, but only validated for certain points globally, such as the drifting buoys and research vessels mentioned previously (Merchant, et al., 2014a). The ocean however, has many local variations that we are still trying to understand and detect. Therefore, it has to be taken into account, that the optimal interpolation that was applied to this data set, can be further improved. The accuracy detection of this study highlighted some areas of improvement, while a larger-scale study could give even more significant results.

As for the utility of the buoy data and satellite data record, one major difference is that buoys require regular maintenance, which is expensive, and have a lower spatial coverage, while satellite data requires higher initial costs and offers a global spatial coverage, which is important for establishing a climate data record.

Other potential sources of error have to be accounted for. Firstly, the median was used as a measure of SST, because the data was assumed to be non-parametric and therefore less affected by outliers. If, by any case, the data was found to be more normally distributed, the mean would be a more appropriate measure of the average. Secondly, the associated uncertainty with each data set, the standard deviation (SD) used for the satellite sensor data and the interquartile range (IQR) used for the buoy data set, both indicate the variability within each of the datasets. In statistical analyses the standard deviation is used in conjunction with the mean, while the interquartile range is used in conjunction with the median. The ESA SST CCI data set however, released the dataset as a median SST measurement with an associated uncertainty given by the standard deviation (Merchant *et al*., 2014a). It was assumed that this was done to achieve a more powerful measure of variability of the satellite data due to the standard deviation considering all values within the data and representing the amount by which every value within the dataset varies from the mean, while the interquartile range ignores outliers. Hence, there is some inconsistency within the statistical analysis, which may have been a source of error. Resulting from that, the IQR was used as a measure of variability for assessment of the buoy data set, in order to comply with standard statistical analysis practice.

Another potential source of error relates to the difference in depth at which the SST measurements were taken. As highlighted in Fig. 1, the satellite sensor ensemble resulted in a SST measurements corresponding to a depth of 20cm ($SST_{sub\text{-}skin}$), while the buoy recordings corresponded to a depth of approximately 1 m (SST_{depth}). The satellite sensor is bias-adjusted to effects of diurnal heating; this bias adjustment includes an estimate of the effects of the oceanic thermal skin layer and the vertical near surface thermal stratification (Merchant, *et al*., 2014). Stratification of the sea surface is caused by convective processes, oscillations and wave action (Stansfield, *et al*., 2013). Vertical mixing, which is related to ocean turbulence, air-sea fluxes of heat, moisture and momentum (GHRSST, 2018), as well as heat transport by currents (Deser, et al., 2010), all play a role in not only causing stratification, but seasonal variation. The limitation of this study was to recognise and document these variations, but explain or relate them no further, as research beyond the available timeframe would need to be done.

Considering the sources of potential bias and assuming that this study validated the use of the ESA SST CCI data to be accurate within 0.4 °C correctly, the potential uses need to be highlighted. RSS (2018) found that the accuracy improvement of recent years due to the combined use of infrared-sensors and microwave-sensors has aided tropical cyclone forecasting immensely due to the availability of higher temporal and spatial resolution satellite SST data when predicting storm events. Miguel and Santos (2000, p.7) stated that "SST is among the oceanographic parameters obtained from satellite remote sensing techniques which has the widest and more successful application in defining the distribution, abundance and availability of marine organisms". Their review on application of remote sensing to fisheries suggested, that a combined use of remote sensing and *in-situ* data can improve the detection of fish schools and hence lower costs associated with fuel, the ship crew and ship maintenance. Further, they suggested that the application to aquaculture, in particular environmental data on the water quality and temperature, can aid planning and managing, as well as support the fishery operation. In 2000, Miguel and Santos (2000) pointed out, that the application is limited by the available satellite sensors, data access, data processing and awareness of the remote sensing application possibilities. The potential use of a combined infrared and microwave wavelength product was mentioned. Current technology, 18 years after Miguel and Santos recognised these issues, has been highly improved due to a higher number of satellites operating, better data access, transfer, sync and interpretation and due to available datasets such as the ESA CCI. Hence, if 18 years ago, in 2000, the importance of application to fisheries and aquaculture was recognised, there is even more reason to make use of the globally available satellite sensor data today; particularly because the satellite sensor accuracy is constantly aimed to be improved, as was pointed out in this paper. However, with an increase in higher quality available data, the demands rise, as was highlighted by the study on the effects of warming waters on copepod biodiversity in the North Atlantic done by Beaugrand et al. (2002) that used a SST scale of 0.01 °C increments. For single organism studies such as this, a much more accurate SST product than the GMPE would need to be used. This was further highlighted by two climatic studies on SST effects on ocean circulation have used SST data with an accuracy of 0.1 °C (Czaja and Frankignoul, 1999; Han *et al*., 2016). If the GMPE product could be improved to 0.1 °C, the data could be used for climatic studies.

As for the future of SST data use, several studies have considered novel technologies. Concurrent with the establishing of the GHRSST-PP, the aim for the future uses of SST observations remains, to improve their accuracy and performance further. This includes the increase of temporal resolution to sensors obtaining global images every 6 to 12 hours to aid a long-term record along with the GCOS guidelines and hourly to two hourly for detailed studies on the effects of SST on specific organisms within the marine environment (Donlon, *et al*., 2007). Spatial improvements would increase sensor resolution to below 10 km (Donlon, *et al*., 2007) and ideally within 1 km as is possible through the use of high spatial satellite sensors. The possibility of availing of satellite observations in near-real time has been highlighted by Donlon *et al*. (2007) and would particularly aid weather forecasting during storm events. In extreme circumstances, where marine organisms could be affected by a rapid change in SST, the possibility of having near-real time observations available could potentially minimise negative impacts significantly.

Change detection studies, such as Principal components analysis (PCA) offer the possibility to detect long-term as well as seasonal and local variations within a dataset by comparing 2 or more satellite images (from different sensors or different dates) and correlating each data point (Piwowar and LeDrew, 1995). Areas of low correlation are the areas of interest, as they indicate areas of change. In detail that means, that the first principal component always shows the maximum amount of variation and each successive component shows smaller amounts of variation (Piwowar, *et al*., 2001). Studies, such as the 21-year sea ice analysis of the Northern hemisphere undertaken by Piwowar et al. (2001) using microwave sensors, have shown that the first component indicates long-term variations due to it not being affected by strong localised extremes, the second component corresponds to seasonal change and any higher components correspond to local variations (Piwowar and LeDrew, 1995). Like the regression analysis conducted in this study, PCA examines the correlation of two variables and not their cause and effect relationship (Piwowar, *et al*., 2011). The addition of a PCA analysis to this study would have offered another way to detect seasonal change (through the use of the second principal component) and localised anomalies (through the use of component 3 and above).

The methods used here can be extrapolated to cover a larger area, applied to other SST products or other datasets provided through the CCI project, considering appropriate methodological adjustments are carried out. However, this does not exclude suggestions to improve the methodology as it was carried out in this study. Firstly, areas less susceptible to cloud cover than Ireland, for example, could rely solely on AVHRRs infrared-sensor measurements and hence have a higher spatial resolution of between 1 and 4 km. A higher spatial resolution would improve the validation accuracy significantly, particularly considering that a typical moored buoy takes measurements at the radius of 1 to 2 metres surrounding the buoy (Meindl, 1996), while each pixel of the satellite corresponds to several kilometres of averaged data for that pixel. A second suggestion to enable this analysis to be more accurate would be to assess the complete data set rather than at 5-day intervals over the 2-year period. It was chosen to conduct the assessment at 5-day intervals due to the computing limitations of this study, but a complete assessment of the 2-year period or even a 10-year period could give even more clues about SST changes associated with natural or anthropogenic sources.

5. Conclusions

This paper has validated, that the GMPE product, provided through the ESA SST CCI, is accurate to within 0.18 °C for the M3 buoy location, 0.22 °C for the M6 buoy location, 0.28 °C for the M5 buoy location and 0.85 °C for the M4 buoy location. Overall, satellite observations were found to have lower SST observations, while the buoy data showed a higher variability. Seasonal variability reflected in the satellite sensor and the buoy data. The M4 buoy was found to underestimate SST in summer and overestimate SST in winter and hence found unreliable for validation of the satellite sensor accuracy. However, accuracy assessment for the other buoys showed that the M3 and M5 buoy location match-up points were overall reliable, but found to be less reliable in winter, while the M6 buoy location results showed an uncertain reliability due to the effects of outliers on the data.

The GMPE products' applicability to Irish waters was found suitable for fisheries and aquaculture, while the further improvement of the product, in the future, could potentially allow application to studies on marine organisms.

6. Recommendations

Improving the accuracy of SST products offers many research opportunities and supports the establishment of a reliable, long-term climate data record (CDR). Therefore, further validation with *in-situ* data needs to be undertaken and any algorithms, interpolation techniques or uncertainty factors, applied to the satellite data, adjusted in order to minimise bias and error associated with each observation. Steps like improving current interpolation products such as the OSTIA product are already undertaken and should be continued, in order to build on existing knowledge.

7. Acknowledgements

Dr. Timothy Sullivan and Mr. Rory Scarrott for their scientific guidance. Mr. Declan Dunne for his help with the data processing. The ERI Beaufort Building for hosting me and allowing space and access to conduct my research within a wide group of researchers. ESA for providing the satellite data and CEDA for facilitating access to the data. Mr. Christopher Merchant, the team leader of the ESA CCI Team, for clarification on the data. Met Éireann for providing the buoy data and the Marine Institute for enabling access to the data. MIDA, the Marine Irish Digital Atlas, for providing and facilitating access to their data on the location of the marine buoys.

This thesis received supervisory support through Mr. Rory Scarrott under the remit of the EU H2020 Co-ReSyF project (Grant agreement No 687289). http://co-resyf.eu/

8. References

Atkinson, C.P., Rayner, N. A., Roberts-Jones, J., Smith, R. O., 2013. Assessing the quality of sea surface temperature observations from drifting buoys and ships on a platform-by-platform basis. *Journal of Geophysical Research: Oceans*. 118, pp.3507-3529. doi:10.1002/jgrc.20257

Beaugrand, G., Reid, P.C., Ibanez, F., Lindley, J.A., Edwards, M., 2002. Reorganization of north Atlantic copepod biodiversity and climate. *Science*. 5573, pp.1692-1694.

Bulgin, C. E., Embury, O., Merchant, C.J., 2016. Sampling uncertainty in gridded sea surface temperature products and Advanced Very High Resolution Radiometer (AVHRR) Global Area Coverage (GAC) data. *Remote Sensing of Environment*. 177, pp.287-294.

Brinckmann, S., Trentmann, J., Ahrens, B., 2014. Homogeneity Analyis of the CM SAF Surface Solar Irradiance Dataset Derived from Geostationary Satellite Observations. *Remote Sensing*. 6, pp.352-378.

Cannaby, H., Hüsrevoglu, Y. S., 2009. The influence of low-frequency variability and long-term trends in North Atlantic sea surface temperature on Irish waters. *ICES Journal of Marine Science*, 66, pp.1480-1489.

Czaja, A., Frankignoul, C., 1999. Influence of the North Atlantic SST on the atmospheric circulation. *Geophysical Research Letters*, 26 (19), pp.2969-2972.

Deser, C., Alexander, M.A., Xie, S.-P., Philips, A.S., 2010. Sea Surface Temperature Variability: Patterns and Mechanisms. *Annual Review of Marine Science*. 2, pp.114-143.

Donlon, C., Robinson, I., Casey, K. S., Vazquez-Cuervo, J., Armstrong, E., Arino, O., Gentemann, C., May, D., LeBorgne, P., Piolle, J., Barton, I., Beggs, H., Poulter, D. J. S., Merchant, C. J., Bingham, A., Heinz, S., Harris, A., Wick, G., Emery, B., Minnett, P., Evans, R., Llwellyn-Jones, D., Mutlow, C., Reynolds, R. W., Kawamura, H., Rayner, N. 2007. The Global Ocean Data Assimilation Experiment High-resolution Sea Surface Temperature Pilot Project. *American Meteorological Society*. 88 (8), pp.1197-1213.

EPA, 2016. Climate Change Indicators in the United States: Sea Surface Temperature. [Online] Availabe at: <https://www.epa.gov/climate-indicators> [accessed: 11.03.2018].

GHRSST, 2018. The Group for High Resolution Sea Surface Temperature, Products. [Online] Available at: <https://www.ghrsst.org/ghrsst-data-services/products/> [accessed: 11.03.2018].

GHRSST Science Team, 2010. The Recommended GHRSST Data Specification (GDS) 2.0, document revision 5, available from the GHRSST International Project Office, 2011, pp.123.

Good, S., Rayner, N., 2013. SST CCI Product User Guide, CCI Phase 1 (SST), Project Document SST_CCI-PUG-UKMO-001. [Online] Available at: <http://www.esa-sst-cci.org/PUG/pdf/SST_CCI-PUG-UKMO-201-Issue_1-signed.pdf> [accessed 14.07.2017].

Google Earth, 2017. [Online] Available at: <https://www.google.com/earth/> [accessed: 29.08.2017].

Han, Z., Luo, F., Wan, J., 2016. The observational influence of the North Atlantic SST tripole on the early spring atmospheric circulation. *Geophysical Research Letters*, 43 (6), pp.2998-3003.

Marine Institute, 2018a. The Real Map of Ireland. [Online] Available at: <https://www.marine.ie/Home/site-area/irelands-marine-resource/real-map-ireland> [accessed: 08.03.2018].

Marine Institute, 2018b. Importance of Ireland's marine resource. [Online] Available at: <https://www.marine.ie/Home/site-area/irelands-marine-resource/importance-irelands-marine-resource?language=en> [accessed: 08.03.2018].

Marine Institute, 2018c. Irish Weather Buoy Network. [Online] Available at: <http://www.marine.ie/Home/site-area/data-services/real-time-observations/irish-weather-buoy-network> [accessed: 03.03.2018].

Marine Institute, 2018d. Irish Weather Buoy Network Observations. [Online] Available at: <http://www.marine.ie/Home/site-area/data-services/real-time-observations/irish-weather-buoy-network-observations> [accessed: 20.07.2017].

Maurer, J., 2002. Infrared and microwave remote sensing of sea surface temperature (SST). [Online] Available at: <http://www2.hawaii.edu/~jmaurer/sst/> [accessed: 11.03.2018].

Meindl, A., 1996. Guide to moored buoys and other ocean data acquisition systems, Data Buoy Cooperation Panel, World Meteorological Organization. Intergovernmental Oceanographic Commission (of UNESCO). DBCP Technical Document No.8. [Online] Available at: <https://www.wmo.int/pages/prog/amp/mmop/documents/dbcp/Dbcp8/DBCP-08-Guide-Moored-Buoys.pdf> [accessed: 10.03.2018].

Merchant, C. J., Embury, O., Roberts-Jones, J., Fiedler, E., Bulgin, C. E., Corlett, G. K., Good, S., McLaren, A., Rayner, N., Morak-Bozzo, S., Donlon, C., 2014a. Sea surface temperature datasets for climate applications from Phase 1 of the European Space Agency Climate Change Initiative (SST CCI). *Geoscience Data Journal*. 1, pp.179-191.

Merchant, C. J., Embury, O., Roberts-Jones, J., Fiedler, E., Bulgin, C. E., Corlett, G. K., Good, S., McLaren, A., Rayner, N., Morak-Bozzo, S., Donlon, C., 2014b. ESA Sea Surface Temperature

Climate Change Initiative (ESA CCI SST): Analysis long term product version 1.0. NERC Earth Observation Data Centre, July 2017. doi: 10.5285/878bef44-d32a-40cd-a02d-49b6286f0ea4.

Met Éireann, 2018. The Marine Unit. Marine Buoy Locations. [Online] Available at: <https://www.met.ie/marine/buoy_locations.asp> [accessed: 03.03.2018].

Met Éireann, 2016. Weather News, Science Week 2016: The Irish Buoy Network. [Online] Available at: <https://www.met.ie/news/display.asp?ID=417> [accessed 14.03.2018].

MIDA, 2015. Marine Irish Digital Atlas. Marine Data Buoys. [Online] Available at: <http://mida.ucc.ie/pages/atlas/atlas.php?addLayers=MDBuoys&onLayers=MDBuoys> [accessed: 03.08.2017].

Miguel, A., Santos, P., 2000. Fisheries oceanography using satellite and airborne sensing methods: a review. *Fisheries Research*, 49, pp.1-20.

NOAAASIS, 2017. Advanced Very High Resolution Radiometer – AVHRR. [Online] Available at: <http://noaasis.noaa.gov/NOAASIS/ml/avhrr.html> [accessed: 04.03.2018].

Piwowar, J. M., Derksen, C.P., LeDrew, E.F., 2001. Principal Component Analysis of the Variability of Northern Hemisphere Sea Ice Concentrations: 1979-1999. *Proceedings, 23rd Canadian Symposium on Remote Sensing/ 10e Congrès de L'Association québécoise de télédétection*, Ste.-Foy PQ, August 2001, pp.619-628.

Piwowar, J.M, leDrew, E.F., 1995. Hypertemporal analysis of remotely sensed sea-ice data for climate change studies. *Progress in Physical Geography*, 19 (2), pp.216-242.

Posselt, R., Mueller, R., Stöckli, R., Trentmann, J., 2011. Spatial and Temporal Homogeneity of Solar Surface Irradiance across Satellite Generations. *Remote Sensing*. 3, pp.1029-1046.

Rayner, N. A., Brohan, P., Parker, D. E., Folland, C. K., Kennedy, J. J., Vanicek, M., Ansell, T. J., Tett, S. F. B., 2006. Improved Analyses of Changes and Uncertainties in Sea Surface Temperature Measured In Situ since the Mid-Nineteenth Century: The HadSST2 Dataset. *Journal of Climate*. 19, pp.446-469.

Reynolds, R.W., Smith, T.M., Liu, C., Chelton, D.B., Casey, K.S., Schlax, M.G., 2007. Daily High-resolution Blended Analyses for sea surface temperature. *Journal of Climate*. 20, pp.5473-5496.

RSS, 2018. Remote Sensing Systems, Sea Surface Temperature. [Online] Available at: <http://www.remss.com/measurements/sea-surface-temperature/> [accessed: 05.03.2018].

Stansfield, K.L., Palmer, M.R., Rippeth, T.P., Simpson, J.H., 2013. Turbulent mixing in the seasonally-stratified western Irish Sea: a Thorpe Scale perspective. *Ocean Science*. 10, pp.2141-2155.

STFC, 2011a. SST CCI Product User Guide Quick Start Guide, Issue 1, Quick Start Guide to ESA SST CCI Products. [Online] Available at: <http://cedadocs.ceda.ac.uk/959/1/SST_CCI-QuickStartGuide-Issue-1.pdf> [accessed: 07.07.2017].

STFC, 2011b. Science and Technology Facilities Council, Natural Environment Research Council, Centre for Environmental Data Analysis. [Online] Available at: <http://data.ceda.ac.uk/neodc/esacci/sst/data/> [accessed 07.07.2017].

STFC; 2011c. Science and Technology Facilities Council, Natural Environment Research Council, Centre for Environmental Data Analysis. Index of /neodc/esacci/sst/data/lt/Analysis/L4/v01.1/. [Online] Available at: <http://data.ceda.ac.uk/neodc/esacci/sst/data/lt/Analysis/L4/v01.1/> [accessed: 07.07.2017].

STFC, 2011d. Science and Technology Facilities Council, Natural Environment Research Council, Centre for Environmental Data Analysis. [Online] Available at: <http://data.ceda.ac.uk/neodc/esacci/sst/data/comparison/DailyOI-AVHRR/> [accessed: 27.06.2017].

Veal, K., Corlett, G., 2017. Data Access Requirements Document, SST-CCI-Phase-II. SST_CCI-DARD-UOL-201. [Online] Available at: <http://www.esa-sst-cci.org/PUG/pdf/SST_CCI-DARD-UOL-201-Issue_2-signed.pdf> [accessed: 11.03.2018].

Appendix

Raw Data is available from the following sources.

The Met Éireann buoy data is accessible through:

http://www.marine.ie/Home/site-area/data-services/real-time-observations/irish-weather-buoy-network-observations

The ESA SST CCI GMPE Lv. 4 data is accessible through:

http://data.ceda.ac.uk/neodc/esacci/sst/data/lt/Analysis/L4/v01.1/.